JAERI-M
9301

CLUPH : A FORTRAN PROGRAM OF COLLISION PROBABILITIES FOR HEXAGONAL LATTICE AND IT'S APPLICATION TO VHTR

February 1981

Keichiro TSUCHIHASHI and Yorio GOTOH

日本原子力研究所
Japan Atomic Energy Research Institute

JAERI-M 9301

CLUPH : A Fortran Program of Collision Probabilities for Hexagonal Lattice and its Application to VHTR

Keichiro TSUCHIHASHI and Yorio GOTOH

Division of Reactor Engineering, Tokai Research Establishment, JAERI

(Received January 8, 1981)

A new collision probability routine CLUPH was added to the computer program set LAMP-B to analyse the hexagonal VHTR fuel and control blocks where in addition to the annular array of fuel pin rods the asymmetric insertions of burnable poison rods and control rods are characteristic.

The perfect reflective boundary condition is no more realistic to consider the arrangement of asymmetric hexagonal blocks. The periodic and the rotational arrangement of blocks are surveyed to consider the interference effect between the burnable poison rods. In addition the effects of coated particle fuel in fuel rod, and of B_4C grain in burnable poison rod, are investigated. The average cross sections of control rod block were derived from the calculation of a super cell which consists of the control rod block and of the surrounding six fuel blocks. The care was taken to the control rod block located at the core-reflector boundary by replacing a sector of surrounding material in supper cell by reflector material. The two dimensional diffusion calculations of simplified cores of Mk-III were performed to obtain the reactivity worths of control rods, for illustration.

Keywords : Collision Probability, Computer Program, Hexagonal Fuel Block, Coated Particle, Burnable Poison, Super Cell, Reactivity Worth, VHTR, Reactor Core

JAERI－ M 9301

CLUPH；六角格子の中の衝突確率を計算するプログラムとその高温ガス炉への応用

日本原子力研究所東海研究所原子炉工学部
土橋敬一郎・後藤頼男

（1981年1月8日受理）

衝突確率を計算する，新しい計算ルーチンCLUPHをプログラムセットLAMP－Bに組込んだ。これは，燃料棒の円環状配置に加えて可燃性毒物棒や制御棒の非対称挿入が特徴である多目的高温ガス炉の燃料ブロックおよび制御棒ブロックを解析するためのものである。非対称な六角ブロックの配置を考える時，完全反射条件はもはや現実的ではない。可燃性毒物棒間の相互作用を考慮するため，燃料ブロックの周期的および回転的配置について調べた。また燃料棒の中の被覆燃料粒子と可燃性毒物棒の中のB_4C粒子の影響を明かにした。制御棒ブロックの平均断面積は制御棒ブロックとそれを取り囲む6個の燃料ブロックからなるスーパーセルの計算から導出する。炉心と反射体との境界にある制御棒ブロックについては，スーパーセルの扇状部分を反射体物質で置き換えた。例としてMk－Ⅲ炉心を簡単化したものにつき，二次元拡散計算を行い，制御棒の反応度価値を求めた。

CONTENTS

目　　次

1. Introduction

The design study of the multi-purpose very high temperature gas cooled reactor has been advanced in JAERI.

In the course of the study it has been realized that the severe accuracy is required in the prediction of the reactivity worth of the control rods in the safety aspect and also of the reactivity worth of the burnable poison rods in the fuel management aspect.

To solve the obscurity arising from the asymmetric insertion of the control rods or the burnable poison rods into the graphite block, a geometric sub-program CLUPH is developed and added to the program set LAMP-B to complete the cell calculation by the collision probability method.

We will describe the CLUPH in the chapter 2 as the supplement of the computer code manual JAERI-1259 for the LAMP-B, the data arrangement and the optional use of the component programs in the LAMP-B for the cell calculation of VHTR taking notice of it's physical problems such as the double heterogeneities of the burnable poison rods with B_4C grain and of the fuel rods with coated particle, the effect of the Bragg's cut off of graphite, the validity of the isotropic reflective boundary condition to the fuel block, and the definition of a super cell for the control rod block analysis and in the chapter 3 as a demonstration of the application of the LAMP-B. In the chapter 4 we will describe the numerical result and discussions about our approach to the Mark III design core of VHTR.

Under the design stage of VHTR the validity of our prediction to the Mark III core is not yet proved, however, we will find what are the problems in the reactor physics part and our solution using the LAMP-B in this report.

2. Development of computer code CLUPH

2.1 Explanation of CLUPH

The computer program set LAMP-B[1] contains many geometry routines for the analysis of various lattice cells, which are based on the collision probability method. But these routines are not enough to the core cell analysis of VHTR (very high temperature gas cooled reactor) being developed in JAERI. The standard fuel block in which 4 % enriched Uranium is used and the control rod blocks of VHTR Mark-III core design[2] have the horizontal cross sections shown in Fig.2.1 and Fig.2.2, respectively. The subprogram CLUP in LAMP-B which seems the most promising for the VHTR core cell analysis, is a analysis code for the clustered fuel assembly of ATR (Advanced Thermal Reactor) whose geometry is shown Fig.2.3. The function of the CLUP, however, can not cover the following items needed for the analysis of the VHTR core cells.

1) The diameters of fuel rod, burnable poison rod and control rod are different each other, which coexist in a block of VHTR, whereas only the annular rings of same fuel rods can be treated in the CLUP.

2) The asymmetric insertion of burnable poison rods or of control rods into the block breaks the symmetric condition around the azimuthal angle.

3) Since the strong absorbers; the burnable poison rods are located by the corner of hexagonal block, the validity of the cylindricalized fuel block and of the isotropic reflective condition has to be tested. The interference effect between the burnable poison rods in the neighbouring blocks should be also investigated.

To solve the above problems the CLUP is modified in the following way.

1. Each fuel rod, burnable poison rod and control rod may have different diameters and compositions, but the number of annular division of these rods is unique in a cell.

2. The moderator region which can originally be split into the concentric annuli in the CLUP, can be also divided into the sectors by the lines radiated from the center of the cell (R-θ division).

3. The rods can be split by the lines mentioned above by putting the centers of these rods on the lines.

4. The hexagonal block can be treated exactly.

5. In addition to the isotropic reflective condition on the boundary of cylindrical cell, the periodic and the rotational arrays of hexagonal blocks are considered (see Fig.2.4 a & b). The latter array distributes burnable poison rods as uniformly as possible. In this case as shown in Fig.2.4 b among the six adjacent cells around a center cell, the first and the fourth cell counting from the above cell in counter-clockwise have the same disposition as the center, but the dispositions of the other four cells are obtained by rotating the center cell by 60° degree in view point of the location of the burnable poison rods. In a periodic array of cell shown in Fig.2.4 a , the two burnable poison rods are located by the some corners, but no rod by the other corners. In the rotational pattern shown in Fig.2.4 b, a rod located near the every corner, therefore, the rods are more uniformly distributed in the rotational pattern than in the periodic one.

The subprogram CLUPH which can cover the above mentioned items has been complied into the LAMP-B as a routine which produces the collision probability . The recombination of regions to minimize the computer time and space can be accomplished by assigning to each zone the same region number as done in other routines of LAMP-B. The allocations of the zone numbers in a hexagonal assembly are explained here as an example. A hexagonal assembly is radially divided by RX's into the three radial concentric annuli in Fig. 2.5, though the outermost boundary is a hexagonal. The assembly is divided

also into three sectors by the three lines radiating from the center at the angle SETA's 90°, 210° and 330°, respectively. By the coupling of the division by RX's and by SETA's, the nine radial zones are made. Moreover, the six fuel rods, the six fuel rods and the three burnable poison rods are inserted in the first , the second and the outermost ring, respectively. Their radial and angular locations are specified by RPP's and THETA's. These rods are sub-divided into the inner and outer annular zones by RDP's. The zone number is allocated first from the rods of the innermost ring and furthermore from a rod of the smallest THETA. But, in a rod of annular structure, the earlier zone number is assigned for the inner zone. Thus the zone numbers from 1 to 12 are assigned for the rods on the innermost ring. The three rods out of six on the second ring are crossed by the radiating lines. In these three rods the zone number is assigned in the counter-clockwise way as in Fig.2.5. After the allocation of the three pin rods on the third ring, the three sectors in the center of the assembly are allocated counter-clockwise from the zone number 37 to 39. Then, the next outer radial zones are allocated succeedingly. The case for IDIVP=1 instead of IDIVP=0 to the same geometry is shown in Fig.2.6 where the radii for the radial positions; RPP's work as RX's. Allocation for the pin rod zones is not changed but the radial zones are more sub-divided. The assignment shown in Fig.2.7 is the case of IDIVP=2 to the same geometry where the rod zones are sub-divided by the RPP's into the inner and the outer zones. The zone number 1,2,3 and 4 are assigned to the first rod on the first ring from the inner to the outer parts in view point of the radial position. To the rods crossed by the radiating lines, such as the second, the fourth and the sixth rods on the second ring, the allocation is not changed. In stead of specifying IDIVP=2, the same function is given by inserting the values of RPP's as RX's in the input.

In Fig. 2.8 is shown the case where IDIVP=0 and the value of the second RPP is added into the array of RX's. The rod zones only on the second ring except the three rods on the radiating lines, are sub-divided by the RPP. The similar case is shown in Fig. 2.9 where IDIVP=1 and the RPP for the second ring is added into RX's. In this case for the first and the third ring, the allocation is performed as IDIVP=1, but for the second ring as IDIVP=2. The program allows to divide the rod zone only by the line which crosses the center of the rod. Therefore, when the radial division of an assembly is possible by some RPP's but is impossible by other RPP's without interesting the rod zones, the radial division can be performed by setting IDIVP=0 and adding the corresponding RPP's into RX's.

2.2 Input and Output of CLUPH

INPUT of CLUPH

BLOCK 0 (5H)

PROB 1-5	Program identification to be entered as 'CLUPH'

BLOCK 1 (72H)

TITLE 1-72	Problem identification. The first four letters of TITLE (1) is used as the case label for the read/ write into/from of the PDS file through the process of the source distribution, the neutron fluxes, the homogenized cross section set, etc.

BLOCK 2

1 NR	Number of regions
2 NM	Number of materials for which macroscopic cross sections are specified
3 NG	Number of energy groups
4 NGLAST	Continuation indicator: Enter NGLAST if the output of the first NGLAST groups is already written in unit 20, and then the remaining output is calculated to form the complete one into unit 21 (0 otherwise)
5 IDRECT	Control for directional probabilities =1, isotropic only =2, isotropic and radial components which are used for the anisotropic diffusion coefficients of Behrens / Benoist model in the EDIT program
6 IFORM	Output form of probabilities =0, Pij (from Vi to Vj) =1, Pij/Σ_j

note the RICM accepts only IFORM=0, and the EDIT processes only IFORM=1

7 ITYPE	Problem type =0, Pij only =1, fixed source calc. (only for NG=1) =2, k calculation (only for NG=1)
8 IEDPIJ	Selection of output unit of probabilities IEDPIJ=IPR + ICD + ITAPE IPR=1, print =0, skip

	ICD=2, card punch =0, skip ITAPE=4, write in unit 21 =0, =0, skip
9 ITXEC	Input device of total cross section =0, card =1, PDS file
10 NGR	Order of Gauss approximation for the radial integration over each radial interval divided by RX's
10 NDA	Number of meshes for the angular integration
11 NX	Number of radial division
12 NDPIN	Number of annular division of a pin rod
13 NTPIN	Total number of pin rods
15 IDIVP	Indicator of radial division by RPP's =0, No action =1, RPP's work as RX's to be the boundaries of radial division except the pin rod zones. =2, RPP's works as RX's to be the boundaries of radial division. Moreover, the pin rod zone's are divided by RPP's into the inner and outer zones
16 NZ	Total number of zones
17 IBOUND	Indicator for the outer boundary condition =0, isotropic =1, periodic =-1, rotational =2, vacuum
18 NHEX	Indicator for the shape of the assembly =0, circular =1, hexagonal
19 NCELL	Number of assemblies traced by a neutron path: this item is used in forming the path table. If NHEX=0, NEELL is automatically set to one
20 NTETA	Number of azimuthal division. If NTETA =0 (or=1), no division is taken
21 ICRX	RX(ICRX) is the outer boundary of θ - dependent zones,i.e.,the radial zones where r > RX(ICRX) is not divided by

	the radiating lines even if NTETA > 1 is specified. When this function is not used ICRX should be specified as NX + 1. This item is ineffective in case of hexagonal case.
22 IBETM	Integer number of the range of angular integration by degree. In a general case IBETM=360. If any symmetry exist, it can be reduced. It is noted that the angle of a radiating line which denotes an angular position (division) is measured from the base line which is drawn from the center to across a corner of the hexagon. If any symmetric condition exists about this base line IBETM is reduced to 180. If a periodic condition exists for every 60 degree IBETM can be 60. Specially for the case of NCELL=1 and of the isotropic reflecting boundary condition the range can be reduced to the half of the angular period, if any symmetric condition exists in a period. This item should be carefully chosen because the pitch on the angular integration is decided by IBETM/NDA and the running time is proportional to NDA.

To form the path table, the total $NX^1 * NGR * NDA$ lines are drawn for the radial and the angular integration. NGR=8, IBETM/NDA=5°are recommended (NX^1 is the number of radii RX's modified by RPP's)

23 NRES	Control for debugging Normally enter NRES=0
BLOCK 3	required if NTETA > 1
ISETA (I) I=1, NTETA	The integer angle by degree for the angular division of the assembly. This is immediately transfered into SETA's in radian after reading
BLOCK 4	
NREG (I), I=1, NZ	Region number assigned to the zone I
BLOCK 5 (9A8)	
MATNAME (I), I=1, NM	Member name of the material I; the material number is assigned in the order of input starting at 1; required if ITXEC=1
BLOCK 6	
MAT (I), I=1, NR	Material number assigned to the region I

BLOCK 7

RX (I) I=1, NX + 1	The radii for the radial division of the assembly. RX(1) has to be zero. For a hexagonal case, RX (NX+1) must be the half of the lattice pith (=$\sqrt{3}$/2 times of a side length)
BLOCK 8 RDP (I,J) I=i, NDPIN + 1 J=1, NTPIN	The radii for the annular division of the J-th pin rod. RDP (1,J) has to be zero.
BLOCK 9	
RPP (J), J=1, NTPIN	The radial position of the J-th pin rod The relation must hold RPP (J) $\leq$ RPP(J +1)
BLOCK 10	
THETA (J) J=1, NTPIN	The angular position of the J-the pin rod (in degree). The relation must hold. THETA (J) < THETA (J + 1) when RPP(J) = RPP (J + 1)
BLOCK 11 SIGT (M) Total SIGS (M) Scattering SIGF (M) Fission	required only if ITXEC=0 and NG=1 cross sections for material M. A new card is required for each material
BLOCK 11	required only if ITXEC=0 and NG > 1
SIG (N,M) N=1, NG, M=1, NM	Total cross sections. A new card is required for each material
BLOCK 12 S(I) I=1, NR	required only if NG=1 and ITYPE=1 Fixed source distribution per unit volume

OUTPUT of CLUPH

We describe the output of CLUPH which is common among the collision probability programs in the LAMP - B

A. LIST

1 INPUT data from card

2 Radii, RX's including RPP's which act as RX

3 Volume for each zone

4 Volume for each region

5 Number of paths drawn and the elapsed time for completing the path table

6 Ratios of numerically integrated volumes by region to analytic ones. The formers are calculated as
Vi (numeric)= $\iint d\rho d\phi t_i$
where t_i is the cut of region i by a path. The deviations of these ratios from unity should be kept within a few per cents. The big deviation often occurs at the region whose area is only a small fraction of the whole area because the region is crossed by relatively few lines defined by ρ and ϕ. On the contrary so far as all deviation is kept less than 1.0 %, NGR and NDA can be reduced to economize the computer time.

7 If required [P (vi→vj) for j=1, NR and P (vi→OUT)] for i=1, NR

8 If the directional probabilities are required $\underset{j}{\text{Sum}}\ [P(vi \rightarrow vj)\ /\Sigma_j]$ for i=1, NR
Items 7 and 8 are repeated for g=1, NG

9 The result of one group calculation is printed if required. (See detail in p 34. JAERI-1259)

B. PUNCH

1 TITLE

2 MAT (I), I=1, NR

3 VOL (I), I=1, NR

4 P (vi→vj, g), j=1, NR, i=1, NR,

5 If the directional probabilities are required
DR_{ig} (= Sum $Pij/\Sigma j$) i=1, NR
Item 4,5 are repeated for g=1, NG

C. F21

1 LABELED COMMON / LAMPC/ 997 words

2 P (vi→vj, g), i=1, NR, j=1, NR

3 If the directional probabilities are required
DR_{ig} i=1, NR
Item 2,3 are repeated for g=1, NG

3. Scheme of Calculation

3.1 Cross sections

3.1.1 Thermal cross sections

The 30 group energy structure is shown in Table 3.1. The fission and capture cross sections of each nuclide are obtained from ENDF/B-IV[3] file by the series codes THERMOFILE, THERMOLIB and THERMOSEC.[4] The scattering matrices

6 Ratios of numerically integrated volumes by region to analytic ones. The formers are calculated as
Vi (numeric)= $\iint d\rho d\phi t_i$
where t_i is the cut of region i by a path. The deviations of these ratios from unity should be kept within a few per cents. The big deviation often occurs at the region whose area is only a small fraction of the whole area because the region is crossed by relatively few lines defined by ρ and ϕ. On the contrary so far as all deviation is kept less than 1.0 %, NGR and NDA can be reduced to economize the computer time.

7 If required [P (vi → vj) for j=1, NR and P (vi → OUT)] for i=1, NR

8 If the directional probabilities are required $\underset{j}{\text{Sum}}\ [P(vi \rightarrow vj) / \Sigma_j]$ for i=1, NR
Items 7 and 8 are repeated for g=1, NG

9 The result of one group calculation is printed if required. (See detail in p 34. JAERI-1259)

B. PUNCH

1 TITLE

2 MAT (I), I=1, NR

3 VOL (I), I=1, NR

4 P (vi → vj, g), j=1, NR, i=1, NR,

5 If the directional probabilities are required
DR_{ig} (= Sum Pij/Σj) i=1, NR
Item 4,5 are repeated for g=1, NG

C. F21

1 LABELED COMMON / LAMPC/ 997 words

2 P (vi → vj, g), i=1, NR, j=1, NR

3 If the directional probabilities are required
DR_{ig} i=1, NR
Item 2,3 are repeated for g=1, NG

3. Scheme of Calculation

3.1 Cross sections

3.1.1 Thermal cross sections

The 30 group energy structure is shown in Table 3.1. The fission and capture cross sections of each nuclide are obtained from ENDF/B-IV[3] file by the series codes THERMOFILE, THERMOLIB and THERMOSEC.[4] The scattering matrices

of concerned nuclei except graphite are calculated by the free gas model. For graphite the scattering law data in ENDF/B-III[5] are introduced into the subprogram PIXSE for energy and angular integration. The coherent elastic cross sections calculated by the HEXSCAT[6] are added to the matrix, and the effect of the incoherent approximation to these cross sections which are calculated in the PIXSE, is also investigated. The scheme to organize the library is illustrated in Fig.3.1.

3.1.2 Resonance Parameters

The resolved resonance parameters are retrieved from the ENDF/B-IV file to prepare the temperature dependent cross sections in the subprogram LTE . From the same data file, the file 3 data (back ground cross sections) are retrieved and fed into an auxiliary program SMOOTH to calculate the additional multi-group cross sections to the result of the resonance integral.

3.1.3 Fast neutron cross sections

The energy group structures of the fast neutron library are shown in Table 3.2. The standard library of LAMP-B carries the data for 33 nuclei in which there are duplicate sets for O-16, AL-27, U-235, U-238, PU-239, PU-240, PU-241 to keep sets coming from the GAM-II library[7] and the revised sets.

3.2 Cell calculation in thermal range

The scheme to execute the cell calculation in the thermal range is illustrated in Fig.3.2. We describe briefly the function of the component subprogram. The PIXEDT composes the macroscopic cross sections and the source distributions of the constituent materials using the thermal microscopic library, and put them into a PDS output file. Any of routines PATH, CLUPH yields the collision probabilities. The PIJF solves the linear equations for the neutron fluxes by an iterative method. The EDIT produces the cell averaged macroscopic cross sections in the same format as those of com-

ponent materials. As shown in Fig. 3.3 a series of the above routines are used doubly to solve the double heterogeneous effect due to the burnable poison rods which are composed of the B_4C grains dispersed in the graphite binder. A smearing process by assuming a spherical cell surrouding a grain, leads to 30 group set of the burnable poison rods.

3.3 Resonance Integral

The routine CLUPH used in the thermal range also prepares a table of the collision probabilities to cover the possible variation of resonance cross section. The routine PRERI supplies the macroscopic collision cross sections to the CLUPH, which are kept constant, except the resonant material to be able to interpolate the collision probabilities by one variable.

The separate run of a program SMOOTH to the File 3 data of ENDF/B-IV for U-235 and U-238 prepares the additional cross sections to the effective resonance cross sections

The routine RICM reads the composition and several control parameters from the SYSIN file, the tabulated collision probabilities from an output file of CLUPH, and the sequential arrays of microscopic cross sections from an output file of LTE, respectively. The RICM solves the linear equations to get neutron flux of every fine energy point where the collision probabilities are obtained by interpolation from the tabulated values. The microscopic cross sections multiplied with fluxes are integrated by energy group of the fast library to lead the resonance integrals. Finally the smooth and the P_1 components which do not vary by temperature are added to the effective cross section. To get the effective cross sections in this step there are two ways: one is simply to divide the group integrals by the lethargy width by assuming the flux spatially flat and the 1/E spectrum, the other is to divide them by the integrated fluxes over space and energy, which have the local depression due to the resonance absorption. The former will cause a under-estimate

of absorption in the multigroup calculation where the depression of the group fluxes occurs because of the effective absorption cross sections, while the reaction rate is preserved if the depression does not occur. In this view point the latter process seems resonable, however, there is no assurance that the depression appearing in the resonance integral calculation is reproduced in the multigroup calculation.

In the above discussion the geometrical treatment was fixed to use the collision probability routine CLUPH . The adaptability of a simpler model is also investigated by assuming a circular pin rod cell in an assembly surrounded by equivalent amount of graphite.

3.4 Cell calculation in fast range

The scheme to obtain the fast and epithermal cross sections uses the EPISPEC routine in Fig 3.4. The EPISPEC calculates the spectrum of homogenized system and homogenized cross sections by considering the fast fission effect and the resonance shielding effect. From the information in the fast fission energy region obtained by the PIJF, only flux distributions are applied to the EPISPC to smear the lattice but the energy spectrum of the fluxes is recalculated. The effective absorption and fission cross sections of the resonance region are used to replace the corresponding data in the fast libraly.

3.5 Double heterogeneity due to B_4C grains in burnable poison rod

The burnable poison rod of VHTR is formed by B_4C grains of diameter 600 μ dispersed in graphite binder. Because of the strong absorption of ^{10}B in the thermal neutron range, the self shielding of B_4C grains to graphite binder occurs (microscopic heterogeneity), and the self-shielding of the burnable poison rod in the graphite block also occurs (macroscopic heterogeneity).

We take an additional cell calculation process to solve the microscopic heterogeneity as follows. A spherical cell is assigned for a B_4C grain surrounded by equivalent amount of graphite binder. By using a collision probability routine PATH which treats the spherical cell, a set of neutron fluxes of two regions and of 30 groups is obtained by the routine PIJF by giving a temporary distributed source instead of a boundary source coming from the outer surface. In such a strongly absorbing system the neutron spectrum depends on the source distribution. We take only the spatial distribution from the result of the PIJF to average the cross sections of the spherical cell. By the routine EDIT a complete set of the homogenized cross section is formed in the same format as the output of the PIXEDT which yields the macroscopic cross sections of homogeneous material.

3.6 Double heterogeneity due to UO_2 coated particles in fuel rod

A coated particle consists of a fuel kernel of UO_2 with an 500-μm diameter and several layers of pyrocarbon and SiC. Such coated particles, together with a graphite binder, are formed into an annular hollow fuel rod that are inserted into a graphite block. Hence the gigantic resonance cross sections of fuel materials are self-shielded through the microscopic grain structure and the macroscopic rod configuration.

Several works deal with neutron resonance absorption in the material with a grain structure[8-13]. In a simple treatment,[8,9] the individual grains are considered as the fundamental elements, which are assumed to be randomly distributed. Then, the microscopic heterogeneity can be treated by an equivalent spherical two-region cell with an isotropic reflective boundary condition. The effects of particle size distribution[11] and of particle spacing[12] were independently investigated by assuming their proper distribution functions. Both studies seems to show that a simply averaged cell is sufficient to take account of the dispersion of sizes and spacings for

resonance absorption in materials with grain structure. A simplified method based on the intermediate resonance approximation is proposed[13] to deal with the present problem. First, a fuel rod with grain structure is homogenized by introducing an equivalent homogeneous material, in the form of an intermediate approximation that contains a fictitious moderator substituted for both the grain and the moderator region. Second, the same approach is also applied to the rod configulation assuming the hollow cylindrical cell instead of the cluster configurations. The good result suggests that the use of the "table look-up" method of resonance shielding factors is helpful.

Taking note of the result of the first step, we consider the cluster configuration of the homogenized rods using the collision probability routine CLUPH.

3.7 Average cross section of control rod block and core calculation by CITATION

The core configuration of VHTR is shown in Fig.3.5. The control rod block in the center of core and of the first ring are surrounded by the six fuel blocks. It can be looked as a super cell which is composed of a control rod block and of the six neighboring fuel blocks. The control rod blocks of second and of third ring locating at core-reflector boundary are adjacent to three and to one fuel block, respectively. The CLUPH has the option to analyze such a cell by assuming for the hexagonal control rod block a cylindrical block with an equivalent section area. Each fuel block or graphite block which surrounds the control rod block, corresponds to a sector of annuli in the super cell. The smeared cross sections of the surrounding fuel block in thermal and in fast energy range should be prepared in advance to the analysis of super cell, which are assigned as a material to a sector. The average cross sections of

control rod block are calculated in the control rod block only after the analysis of super cell. Changing the number of control rods inserted in the block, the average few group cross sections of the various states of the control rod block can be obtained.

The core calculation is performed for instance by the code CITATION of the two dimensional triangular mesh, by assigning the averaged few group cross sections which are obtained by the cell analysis to each block in core. In the calculation of the few group cross sections of reflector graphite, the effects of neutron leakage and of neutron current from the surface of core are considered by performing a multigroup one dimensional core calculation.

4. Application of CLUPH in reactor calculation of VHTR

4.1 Description of MK-III reference core

In the reference core design MK-III of the experimental multi-purpose very high-temperature gas cooled reactor (thermal output 50 MW with reactor outlet gas temperature 1000°C) the fuel is average 4% enriched uranium in the oxide form; fuel element is a prismatic graphite block of hexagonal cross-section containing the hollow fuel pins sheathed in graphite sleeve. The active core consist of 73 vertical fuel columns in 7 tiers arranged in a cylinder of effective diameter 2.7 m and hight 4 m. The reflector elements surround the active core. The reactivity is mainly controlled by 38 control rods driven by the mechanisms in standpipes above the reactor vessel. The coolant He gas flows from the top to the bottom. The enrichments of uranium in fuel block used in upper, middle and lower part of MK-III core are 6, 4 and 2 %, and the numbers of burnable poison rods in the blocks are 3, 2 and 1, respectively.

As the design study of VHTR has been advanced, the evaluation of the precision of design has become important. For example, the design of reac-

control rod block are calculated in the control rod block only after the analysis of super cell. Changing the number of control rods inserted in the block, the average few group cross sections of the various states of the control rod block can be obtained.

The core calculation is performed for instance by the code CITATION of the two dimensional triangular mesh, by assigning the averaged few group cross sections which are obtained by the cell analysis to each block in core. In the calculation of the few group cross sections of reflector graphite, the effects of neutron leakage and of neutron current from the surface of core are considered by performing a multigroup one dimensional core calculation.

4. Application of CLUPH in reactor calculation of VHTR

4.1 Description of MK-III reference core

In the reference core design MK-III of the experimental multi-purpose very high-temperature gas cooled reactor (thermal output 50 MW with reactor outlet gas temperature 1000°C) the fuel is average 4% enriched uranium in the oxide form; fuel element is a prismatic graphite block of hexagonal cross-section containing the hollow fuel pins sheathed in graphite sleeve. The active core consist of 73 vertical fuel columns in 7 tiers arranged in a cylinder of effective diameter 2.7 m and hight 4 m. The reflector elements surround the active core. The reactivity is mainly controlled by 38 control rods driven by the mechanisms in standpipes above the reactor vessel. The coolant He gas flows from the top to the bottom. The enrichments of uranium in fuel block used in upper, middle and lower part of MK-III core are 6, 4 and 2 %, and the numbers of burnable poison rods in the blocks are 3, 2 and 1, respectively.

As the design study of VHTR has been advanced, the evaluation of the precision of design has become important. For example, the design of reac-

tivity control system, which is directly connected with the safety of reactor, is very important. The core shutdown reactivity margins for a pair of control rods stuck in the operating time of reactor and that for a pair of rods plus other one rod (three rods) stuck in the refueling time are considered in the design study. It is desirable that the maximum reactivity worth of a control rod is small but the number of control rods which can be inserted in the reactor core, are limited from view point of reactor structure. Accordingly, the maximum reactivity worth of control rod in this reactor is rather large. Although the reactivity compensation of excess reactivity by the burnable poison rod is made as small as possible, yet the worth of burnable poison rods is less than but comparable with that of control rods. Therefore, the burnable poison rods play the important role in the reactivity control. The precise check of the reactivity balance of this reactor is important.

It is common practice in design study to use an approximate calculational method to save the computing time. But, to evaluate its precision, it is needed to use the method which includes the approximation as little as possible. The codes described in the preceeding sections, which are based on the collision probability method, have been developed for this purpose and applied for the MK-III core calculation.

4.2 Cell analysis of fuel block in thermal energy range

The configuration of fuel block and of control rod block are shown in Fig. 2.1 and 2.2, respectively. The fuel compacts of hollow cylindrical pellet which are made of the coated fuel particles dispersed in the graphite binder, are sheathed in a graphite sleeve. The coated fuel particle of diameter 920μ consists of a fuel kernel of diameter 500μ coated with pyrocarbon and silicon carbide. The volume packing fraction of the coated fuel particles in the graphite binder is 30 v/o. The small holes of diameter

10 ϕ are prepared in the graphite block, in which the burnable poison rod of diameter 8 ϕ can be inserted. The diameter of B_4C kernel in the rod is 600μ and the density of B_4C in the rod is 4.5 w/o. But the specification of the burnable poison is not fixed. The control rod block has three holes of diameter 104 ϕ and three fuel rods. The two of the holes are for the control rods and the one is for the reserve shutdown system which inserts B_4C balls by gravity for emergency. The control rod is a sintered mixture of B_4C and graphite powder, whose inner and outer diameter are 55ϕ and 85ϕ, respectively. The density of boron is 30 v/o. The region maps of the lattice cell of MK-III core, which use 4% enriched uranium, are shown in Fig. 4.1. In the hexagonal lattice, the flight path of neutron is traced over the adjacent hexagonal fuel blocks and the isotropic reflective condition is not used as used in the cylindrical approximation of fuel block whose region map with two burnable poison rods is shown in Fig.4.2. The thermal fluxes calculated in the hexagonal lattices and in the cylindrical approximation for the three kind of fuel blocks are given in Fig.4.3, 4.4 and 4.5, respectively. The flux in the burnable poison rod is about a half of the flux of surrounding region. The flux in fuel rod is a little lower than that in graphite. The cell constants for the three kind of fuel block which were calculated for the hexagonal lattices and for the cylindrical cells, are given in table 4.1, 4.2 and 4.3, respectively. The two kind of graphite cross sections, in coherent and in incoherent approximation were used there, which will be explained later. HEXIB and CLYIB mean the hexagonal cell and the cylindrical cell with a burnable poison rod, respectively. There is no marked difference between the calculated results, but for the three kind of fuel blocks the values of ηf calculated in the hexagonal cells are always larger than that in the cylindrical cells. Particularly in the fuel block with the

three burnable poison rods the ηf in table 4.3 calculated by the hexagonal cell is 0.89% larger than that by the cylindrical cell.

Since the burnable poison rods are inserted near the cell-boundary, the interference between the burnable poison rods of adjacent fuel blocks should be considered. In the hexagonal lattice cell analysis the position of burnable poison rod can be precisely considered. For the standard fuel block which contains 4% enriched uranium and two burnable poison rods, the periodic and the rotational disposition of burnable poison rods in the core lattice can be considered as in Fig.2.4. The thermal flux obtained by using these distributions are compared in Fig 4.6, where in case of the rotational, the flux in the regions by the cell boundary is rather homogeneous except the one in the region surrounding the burnable poison, but in case of periodic distribution the flux in the region which does not surround burnable poison rod but is adjacent to the two rods of neighboring fuel blocks, is reduced. The thermal cross sections of fuel block by the periodical and by the rotational distribution of burnable poison rods are compared in Table 4.2 [HEX2B-COHERENT and HEX2B ROTATIONAL-COHERENT], though they are almost the same, where HEX2B means the hexagonal cell with two burnable poison rods and COHERENT means the coherent elastic cross section of graphite.

Two kinds of graphite cross section are prepared; the one contains the coherent elastic cross section which was calculated by HEXCAT code by considering the crystal structure of graphite and has the Bragg's cut off in the low energy region, and the other has the elastic cross section calculated in the incoherent approximation but has not the Bragg's cut off. Since many absorbing materials are present in the fuel block, the thermal neutron spectrum in the very low energy range has not much contribution. Therefore, the average cross sections of fuel block are not much different each other notwithstanding the different graphite cross sections used in the cell analysis, as can be seen in Table 4.1 and 4.2 except the diffusion coefficient which includes an appreciable contribution in the low energy region.

The effect of burnable poison kernel of diameter 600μ in the burnable poison rod is investigated. In the VHTR design the absorbing grains of diameter 600μ are mixed with graphite binder at the weight percent of boron to carbon by 4.5 w/o. The grain effect is surveyed by changing the mixing ratio of boron to carbon in the grain from the homogeneous limit to the pure B_4C, while the number density of grains are adjusted to keep the constant boron content. Since the weight percent of carbon 4.5 w/o, the following relations can be obtained.

$$\rho_B \frac{V_1}{V} = 4.26 \times 10^{-3}$$

$$\rho_{c1} \frac{V_1}{V} + \rho_{c2}(1 - \frac{V_1}{V}) = 0.08145$$

where V_1, V_2 and $V=V_1+V_2$ denote the volume of grain, of the graphite binder and of the equivalent cell, respectively; ρ_B, ρ_{C1} and ρ_{C2} denote the atomic density of boron, of carbon in the grain and of carbon in the graphite

binder, respectively. Furthermore, the following condition for the density of boron ρ_B is imposed for convenience.

$$\rho_{C_1} + \rho_B = 0.08145$$

because for fixed V_1 all the densities of carbon and of boron are determined as a function of equivalent cell volume V from these relations. For the spherical cell analysis to the burnable poison kernel, the PATH code was used, and the average absorption cross sections obtained for the equivalent cell are compared with the homogeneous absorption cross sections. As the radius of the equivalent cell increases, the shielding effect becomes dominant. With this cross sections for the burnable poison rod, the cell analysis of the hexagonal standard fuel block was performed, and the results are shown in Table 4.4.

When the radius of equivalent cell is small, the lattice constants do not much differ from the corresponding ones in table 4.2, which were calculated without regards for the grain structure of burnable poison, but for the large radius of equivalent cell the differences are dominant and the spherical cell analysis of burnable poison kernel is needed.

4.3 Cell analysis of fuel block in fast energy range

The method to obtain the overall homogenized fast cross section of fuel block is the use of the EPISPEC in the scheme of Fig.3.4. This method precisely consider the heterogeneous effect of fast fission. The top 20 energy group cross sections in 66 energy groups of the fast energy range, are reduced to 10 energy group cross sections by collapsing in the FAXEDT. After the cell calculation about this fast 10 energy groups, the fluxes obtained and the information about the lattice are fed into the EPISPEC. The cross sections of the fast libraly are used in the remaining energy groups except those of resonance energies which are obtained in the resonance integral calculation. Assuming that the flux is spatially flat in the remaining energy range, the energy spectrum is calculated. By using these

spectra, the homogenized multi-group and the collapsed few group cross sections are obtained.

4.4 Infinite medium multiplication factor and its temperature dependence

By combining the results of the cell calculation aboyt thermal and fast neutron, infinite medium multiplication factor k_∞ is obtained for the fuel block. The factor for the fuel blocks which use 2 w/o, 4 w/o and 6 w/o enriched uranium, are 1.11, 1.19 and 1.20, respectively. Since VHTR is operated at from the room temperature to over 1000°C, the cell calculations of the standard fuel block with 4 w/o enriched uranium, were performed at 400°k, 800°k and 1200°k, respectively. The average thermal constants are given in Table 4.5.

The LTE was used to prepare the pointwise resonance cross sections for the RICM at each temperature. The resonance integrals of uranium 238 for 300°k, 400°k, 800°k and 1200°k are 47.53, 49.33, 55.17 and 59.74 barn, respectively. The infinite medium multiplication factor k_∞ decreases compared with that at 400°k, by factor 0.944 and 0.912 at 800°k and at 1200°k, respectively.

4.5 Cell analysis of control rod block and average cross sections of reflector graphite

The control rod block surrounded with six fuel blocks in VHTR core can be regarded as a super cell as can be seen in Fig.3.5. The typical region map for the cell calculation is shown in Fig.4.7. The homogenized cross sections of the surrounding fuel block were prepared in advance as mentioned in the previous sections. The surrounding cylindrical region is subdivided as the width is as half of the thermal neutron free path length. In the resonance energy region, the cross sections of the three fuel rods in a control rod block were replaced by the ones obtained in the resonance

integral calculation. After the cell calculation the homogenized and the collapsed cross sections of the control rod block are obtained. The infinite medium multiplication factor k_∞ of the super cells involving the control rod block with two control rods, with a control rod, and without control rod, are 0.78, 0.94 and 1.21, respectively. The average cross sections of control rod block are calculated from the data within the control rod block, which are obtained by the super cell analysis. So called the second and the third ring control rod blocks by reflector are adjacent to one and to three fuel blocks, respectively. By assigning the suitable regions in the surrounding medium, for the homogenized fuel blocks and for the graphite reflector blocks, the average cross sections of this kind of control rod block can be calculated. The number of fuel blocks which are adjacent to these control rod blocks, is averaged two for a control rod block in the actual calculation.

In the reflector region the neutronic behavior is affected by the neutron leakage from the surface of reactor boundary and by the neutron spectrum of the adjacent fuel blocks. Therefore, to obtain the averaged few group cross sections of the reflector a simple reactor calculation is required. For this purpose the one dimensional diffusion calculation (TUD) was performed, where VHTR loaded with the standard fuel block was treated as a cylindrical reactor. Since the neutron spectrum in the reflector is not much affected by the detailed situation of the reactor core, the following configuration was assumed i.e. from the core center to 109.89cm the super-cell, from 109.9cm to 134.1cm the standard fuel block, from 134.1cm to 239.5cm the graphite reflector. At first, 34 energy groups calculation was performed, where the last energy group is the thermal one group. Then 33-th energy group flux distribution obtained in the preceding calculation is the input of the PIXEDT which calculates the

source distribution for thermal neutron. With this source the thermal 30 energy group calculation was performed to obtain the thermal one group cross section. Only one iteration of this precedure usually is enough to get a few group cross section. The thermal neutron spectra in the graphite reflector are shown in Fig.4.8. The spectrum is so soft that the diffusion coefficients of the coherent cross section is much larger than that of the incoherent approximation.

4.6 Core calculation by CITATION

Using the two group constants obtained by the process described in the previous sections, the core calculations are executed by the CITATION[14] code to investigate the reactivity worth of the control rods.

The configuration shown in Fig.4.9 is a 1/6 sector of the horizontal section of the VHTR. The location of the control block is called as the center (I), the first ring (II) and the outer ring (III, IV) as shown in Fig.3.5. The specification of the calculation is as follows.

Geometry	two dimensional triangle
Zone number per block	6
Mesh number per block	24
Boundary condition	60° rotational, the black absorber beyond the reflector
Problem type	eigenvalue search

All possible combination , irrespective the critical or the subcritical condition, is surveyed by changing the number of control rods inserted in each control rod block but keeping the 60° rotational symmetry around the core axis. The typical neutron flux distribution in the 1/6 sector is shown in Fig.4.10. The changes of K_{eff} associated with the draw of a rod from control rod block, are plotted versus the K_{eff} of initial state are shown in Fig.4.11, 4.12 and 4.13 for the center, for the first ring, and for the second and third ring control rod blocks, respectively. The linear

relations are present in these figures with a few exceptions.

5. Conclusion

As the design study of VHTR has been advanced, it has been recognized that the evaluation of the precision of design calculation is important for the safety of the reactor. Since the maxinum reactivity worth of a control rod and the worth of burnable poison rods which compensate the excess reactivity, are rather large in this reactor, the precise check of the reactivity balance of this reactor is important.

It is necessary to minimize the calculational error caused by the geometrical complexity of the structure. The precisely averaged few group cross sections of fuel and control rod block should be used in the core calculation. For this purpose, the calculational routine CLUPH was made, which is based on the collision probability method and was inserted in LAMP-B program. The CLUPH analyzes the hexagonal cell which may contains several rods of different materials and of different diameters at any position. Not only the radial but also the angular division of the cell are possible. In the hexagonal cell analysis of CLUPH, the isotropic reflective condition at its boundary is not used, but the collision probabilities to the regions of adjacent fuel blocks over the boundary are calculated. In this case the cell patterns in the core can be treated. Starting from a hexagonal cell, two types of cell patterns, i.e., the periodic and the rotational pattern are considered, for a cell with two burnable poison rods, i.e., one by the simple translations of the cell for all three directions in the hexagonal cell and the other by simple translation for a direction, but for the remaining two directions by simple translation plus 60° rotation. By the CLUPH the effect of cell patterns can be estimated, in which the burnable poison rods are asymmetrically inserted. Another option of CLUPH is for the cylindrical cell analysis like in CLUP of LAMP-B, but

relations are present in these figures with a few exceptions.

5. Conclusion

As the design study of VHTR has been advanced, it has been recognized that the evaluation of the precision of design calculation is important for the safety of the reactor. Since the maxinum reactivity worth of a control rod and the worth of burnable poison rods which compensate the excess reactivity, are rather large in this reactor, the precise check of the reactivity balance of this reactor is important.

It is necessary to minimize the calculational error caused by the geometrical complexity of the structure. The precisely averaged few group cross sections of fuel and control rod block should be used in the core calculation. For this purpose, the calculational routine CLUPH was made, which is based on the collision probability method and was inserted in LAMP-B program. The CLUPH analyzes the hexagonal cell which may contains several rods of different materials and of different diameters at any position. Not only the radial but also the angular division of the cell are possible. In the hexagonal cell analysis of CLUPH, the isotropic reflective condition at its boundary is not used, but the collision probabilities to the regions of adjacent fuel blocks over the boundary are calculated. In this case the cell patterns in the core can be treated. Starting from a hexagonal cell, two types of cell patterns, i.e., the periodic and the rotational pattern are considered, for a cell with two burnable poison rods, i.e., one by the simple translations of the cell for all three directions in the hexagonal cell and the other by simple translation for a direction, but for the remaining two directions by simple translation plus 60° rotation. By the CLUPH the effect of cell patterns can be estimated, in which the burnable poison rods are asymmetrically inserted. Another option of CLUPH is for the cylindrical cell analysis like in CLUP of LAMP-B, but

in this case the conditions for rods, for materials and for the division of cell, is the same for the hexagonal cell analysis in CLUPH. This option aimed at the analysis of the control rod block surrounded by the adjacent six fuel blocks, which we deem a super cell. By this newly developed routine CLUPH, the detailed core analysis of VHTR has become possible.

The program developed is applied to the analysis of simplified MK-III-core of VHTR for illustration. The differences are estimated between the hexagonal and the cylindrical cell analysis of fuel block. The difference is 0.9 % of ηf in case of the fuel block with three burnable poison pins. The difference of cell patterns in the hexagonal analysis does not yield the noticeable effects. The selfshielding effect of B_4C grain (600μ mϕ) mixed with graphite binder at the rate of 4.5 w/o yield the depression of 17 % in the absorption cross section of the burnable poison rods from the homogeneous case. It results in the increase of 7 % in ηf value. For the resonance absorption in materials with grain structure, a simplified method based on the intermediate resonance approximation are applied by assigning a fictitious mass and total cross section for the moderator graphite in the fuel rod. The double heterogeneity due to the coated particle, reduces the resonance integral of ^{238}U about 2 barns.

The average cross sections of control rod block are derived from the calculation of the super cell. In case of the control rod block of second or third ring, the homogenized cross sections of fuel block are assigned to a sector of the cylinder surrounding control rod block in the super cell. Considering the effects of the neutron spectrum of the adjacent fuel blocks and of the neutron leakage from the reactor, an one dimensional multi-group core calculation was performed to obtain the average few group cross sections of the graphite reflector. Finally by using the those cross sections of the various blocks, the core calculations with two dimensional

triangular meshes by CITATION were performed for all possible combinations of core configurations which were obtained by changing the numbers of control rods inserted in each control block and by keeping 60° rotational symmetry around the core axis. The mutual interaction between a pair control rods in a control rod block is prominent.

REFERENCES

1) Tsuchihashi K. : "LAMP-B ; A Fortran Program Set for the Lattice Cell Analysis by Collision Probability Method", JAERI-1259 (1979)

2) Aochi T. et al.: " Reference core design Mark-III of the experimental multi-purpose VHTR" JAERI-M-6895 (1976)

3) Kinsey R. : "ENDF/B Summary Documentation", BNL-NCS-17541 (ENDF-201) 2nd Edition (1975)

4) Tsuchihashi K. & Fujita Y. : "A Series of Programs for Processing Thermal Multigroup Constants from ENDF/B Files" (1973) unpublished (in Japanese)

5) Kinsey R. : "ENDF/B Summary Documentation", BNL-NCS-17541 (ENDF-201) 1st Edition (1973)

6) Naliboff Y. D. & Koppel J. D. : "HEXSCAT ; Coherent Elastic Scattering of Neutrons by Hexagonal Lattices", GA-6026 (1964)

7) Joanou G. D. & Dudek J. : "GAM-II ; A B_3 Code for the Calculation of Fast-Neutron Spectra and Associated Multigroup Constants", GA-4265 (1963)

8) Lane R. K. Nordheim L. W. & Sampson J. B.; Nucl. Sci. Eng., 14 390 (1962)

9) Doys M. W. & Pomraning G. C.; Nucl. Sci. Eng., 25, 8 (1966)

10) Wälti P.; Nucl. Sci. Eng., 45, 321 (1971)

11) Jonas H. Hecker R. & Kloth M.; Nucl. Sci. Eng., 58, 89 (1975)

12) Tsuchihashi K. & Gotoh Y.; Nucl. Sci. Eng., 58, 213 (1975)

13) Tsuchihashi K. Ishiguro Y. & Kaneko K.; Nucl. Sci. Eng., 73, 164 (1980)

14) Fowler T. B. Vondy D. R. & Cunningham G. W.; "CITATION ; Nuclear Reactor Core Analysis Code", ORNL-TM-2496, Rev. 2 (1969)

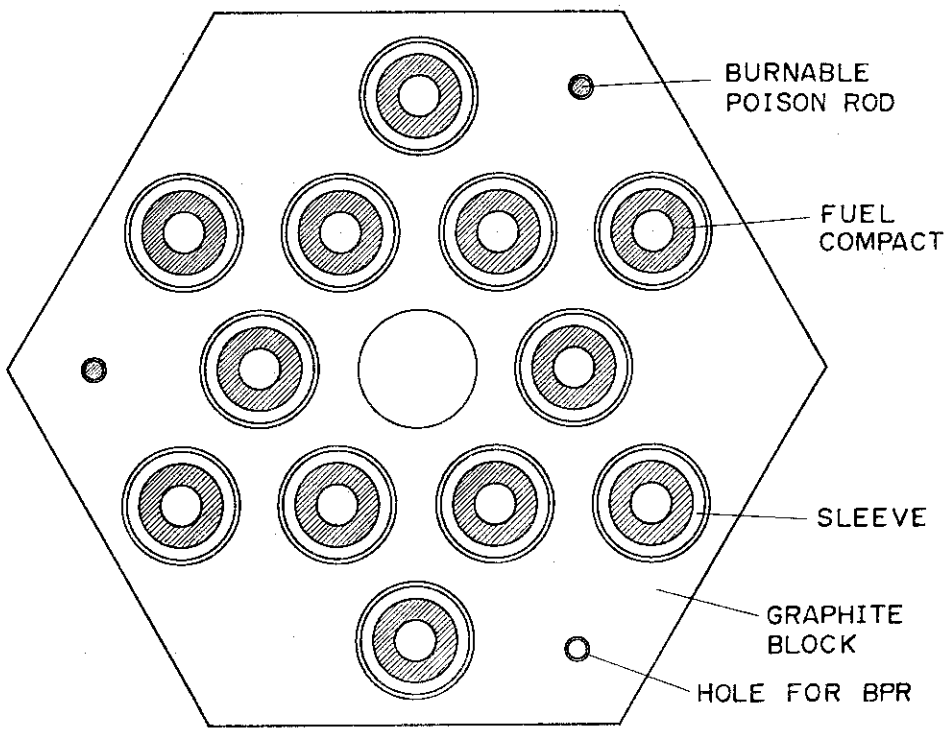

Fig.2.1 Standard fuel block of VHTR.

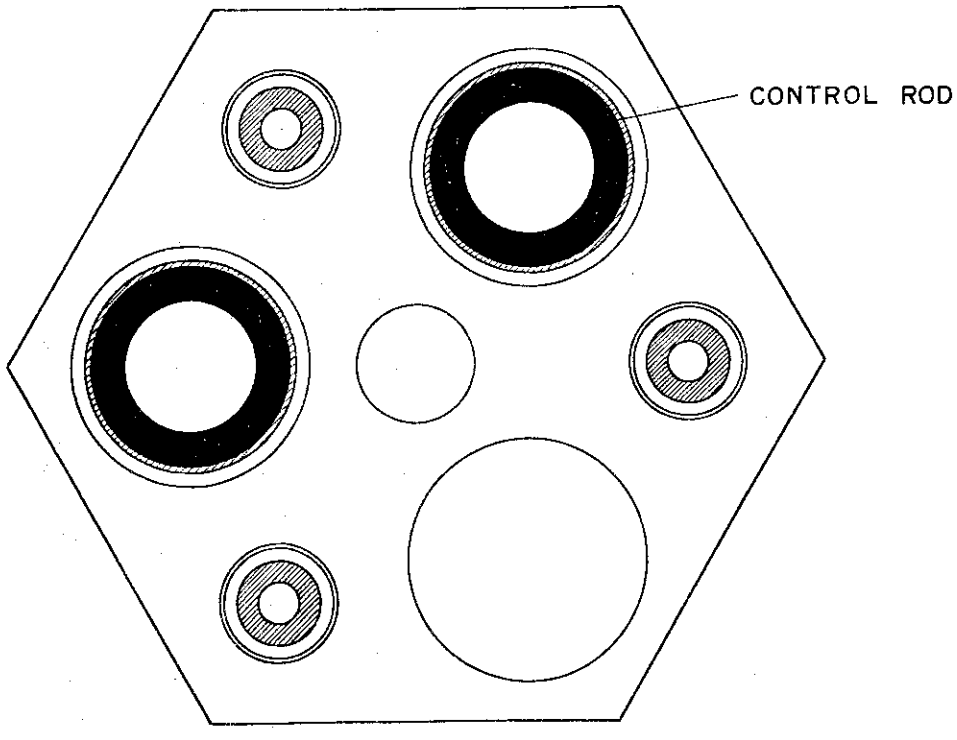

Fig.2.2 Control rod block of VHTR.

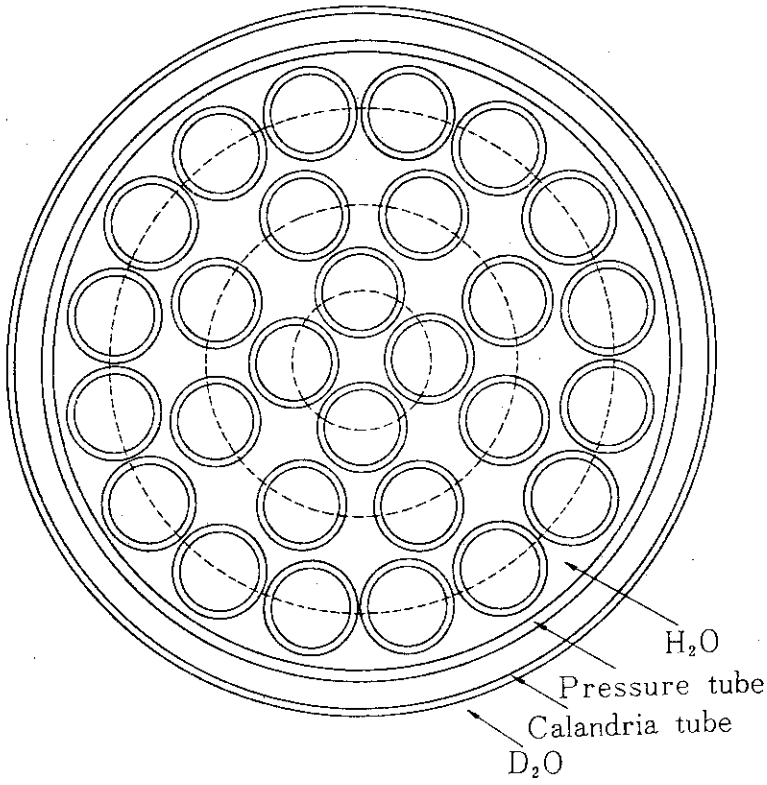

Fig.2.3 Clustered fuel assembly of ATR.

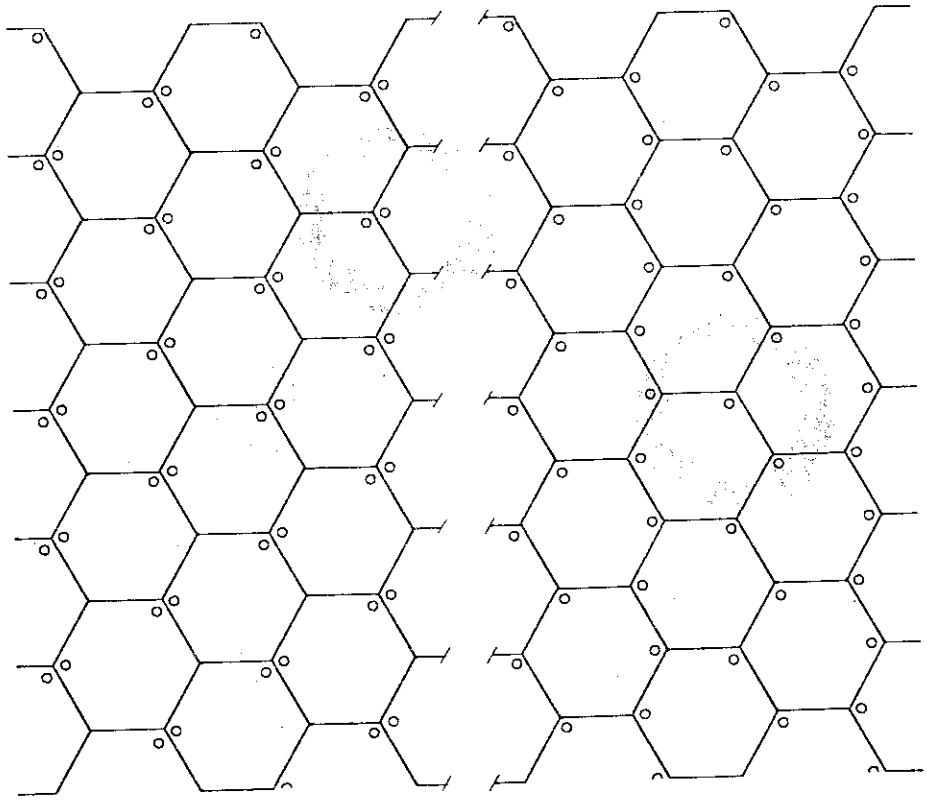

(a; periodic) (b; rotational)

Fig.2.4 Periodic (a) and rotational (b) arrays of hexagonal fuel block with two burnable poison rods.

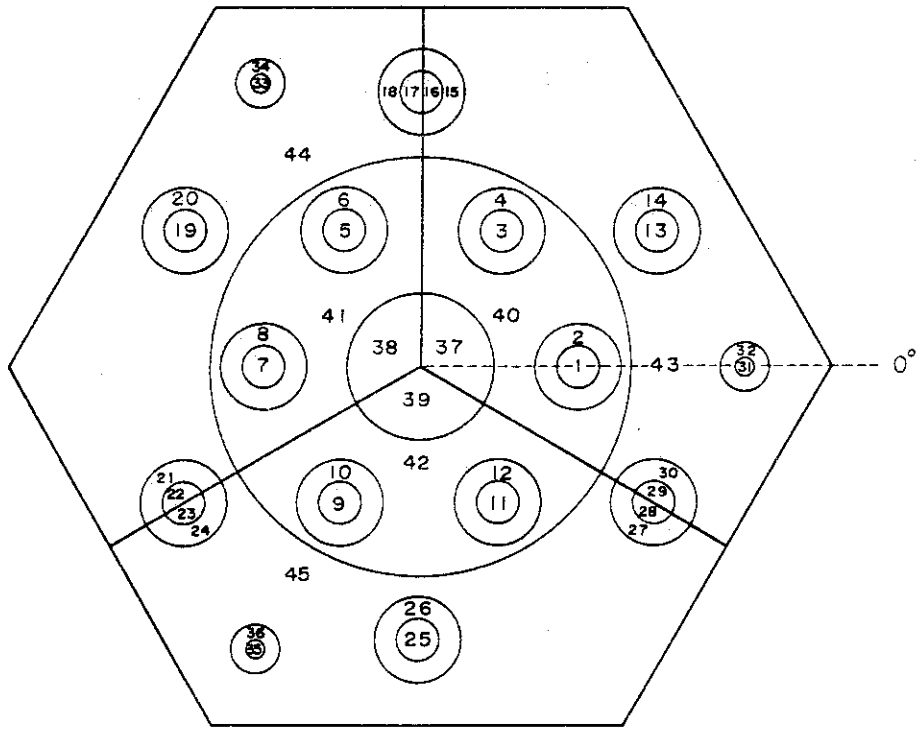

Fig.2.5 Zone map of hexagonal block with RX≒RPP and IDIVP=0.

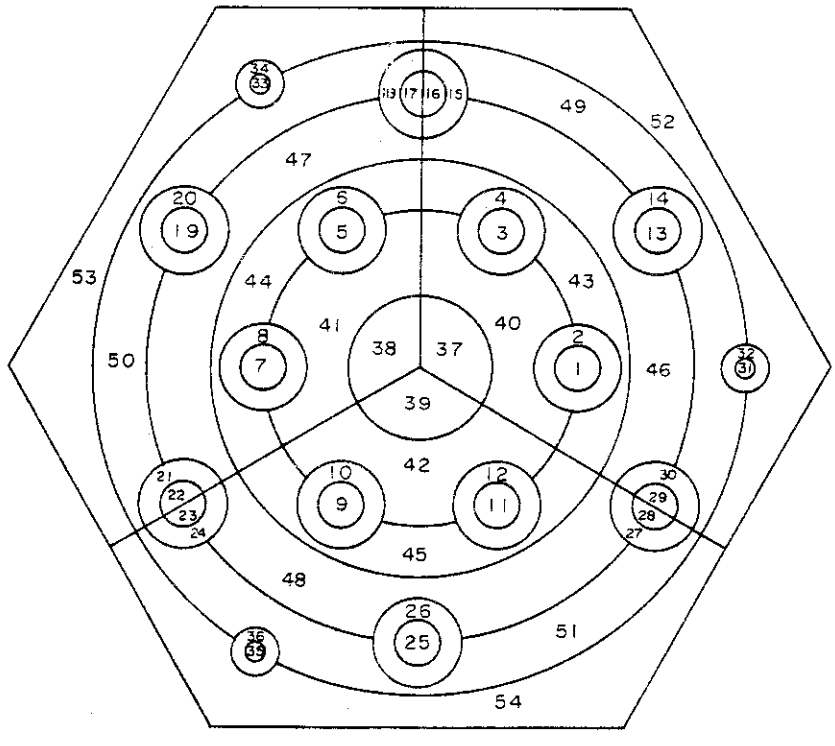

Fig.2.6 Zone map of hexagonal block with RX≒RPP and IDIVP=1.

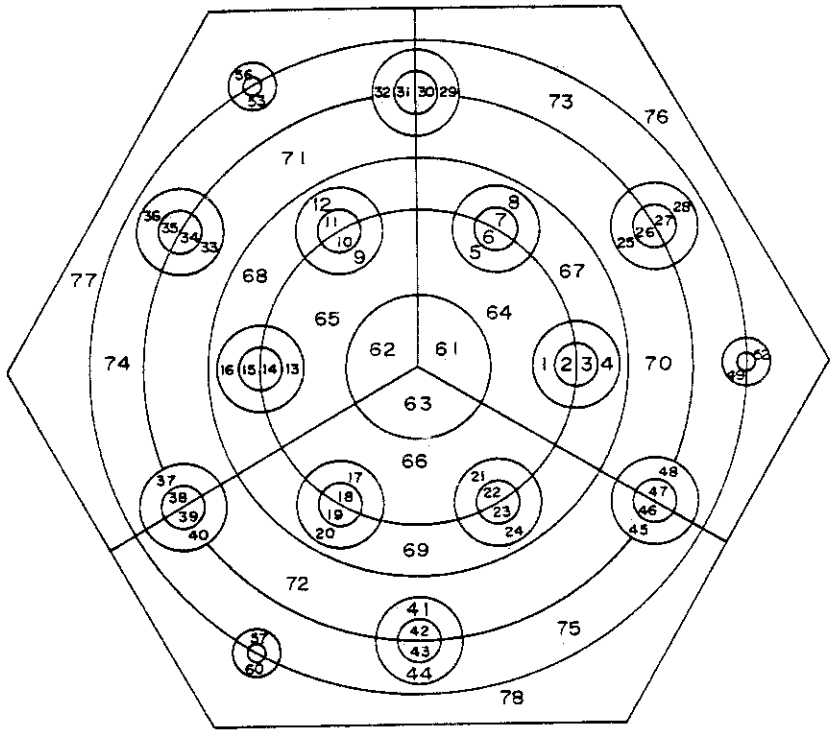

Fig.2.7 Zone map of hexagonal block with RX≠RPP and IDIVP=2.

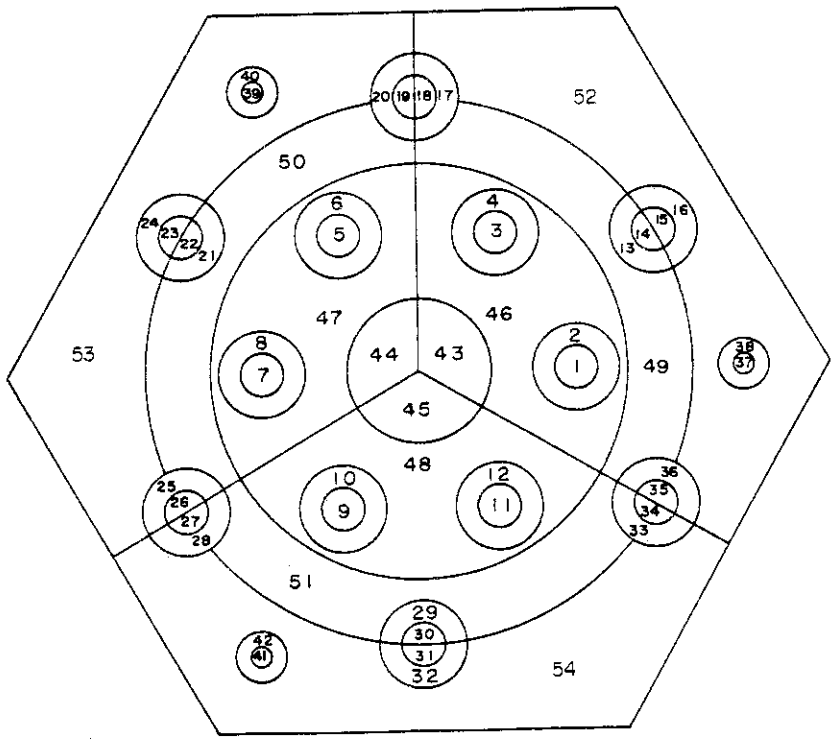

Fig.2.8 Zone map of hexagonal block with RX=RPP and IDIVP=0.

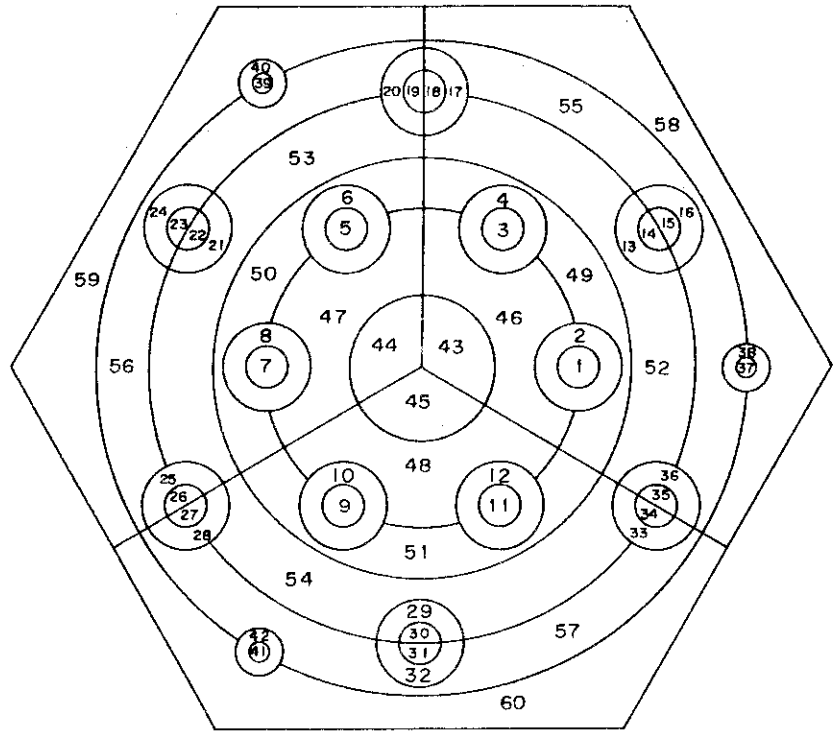

Fig.2.9 Zone map of hexagonal block with RX=RPP and IDIVP=1.

Table 3.1 Energy group structure of thermal neutron.

Group	Lethargy	Max. Energy
1	16,500	6,826E-01
2	16,730	5,422E-01
3	16,960	4,307E-01
4	17,191	3,422E-01
5	17,306	3,050E-01
6	17,421	2,718E-01
7	17,651	2,159E-01
8	17,881	1,715E-01
9	18,111	1,363E-01
10	18,341	1,082E-01
11	18,572	8,599E-02
12	18,802	6,831E-02
13	19,032	5,426E-02
14	19,262	4,311E-02
15	19,492	3,424E-02
16	19,723	2,720E-02
17	19,953	2,161E-02
18	20,183	1,717E-02
19	20,413	1,364E-02
20	20,643	1,083E-02
21	20,873	8,606E-03
22	21,104	6,836E-03
23	21,334	5,431E-03
24	21,564	4,314E-03
25	21,794	3,427E-03
26	22,024	2,722E-03
27	22,254	2,163E-03
28	22,485	1,718E-03
29	22,715	1,365E-03
30	22,945	1,084E-03

Table 3.2 Energy group structure of fast neutron.

Group	Lethargy	Max. Energy
1	0.0	1,000E+07
2	0,500	6,065E+06
3	1,000	3,679E+06
4	1,500	2,231E+06
5	2,000	1,353E+06
6	2,500	8,208E+05
7	3,000	4,979E+05
8	3,500	3,020E+05
9	4,000	1,832E+05
10	4,500	1,111E+05
11	5,000	6,738E+04
12	5,500	4,087E+04
13	6,000	2,479E+04
14	6,500	1,503E+04
15	7,000	9,119E+03
16	7,500	5,531E+03
17	8,000	3,355E+03
18	8,500	2,035E+03
19	9,000	1,234E+03
20	9,500	7,485E+02
21	10,000	4,540E+02
22	10,500	2,754E+02
23	11,000	1,670E+02
24	11,500	1,013E+02
25	12,000	6,144E+01
26	12,500	3,727E+01
27	13,000	2,260E+01
28	13,500	1,371E+01
29	14,000	8,315E+00
30	14,500	5,043E+00
31	15,000	3,059E+00
32	15,500	1,855E+00
33	16,000	1,125E+00

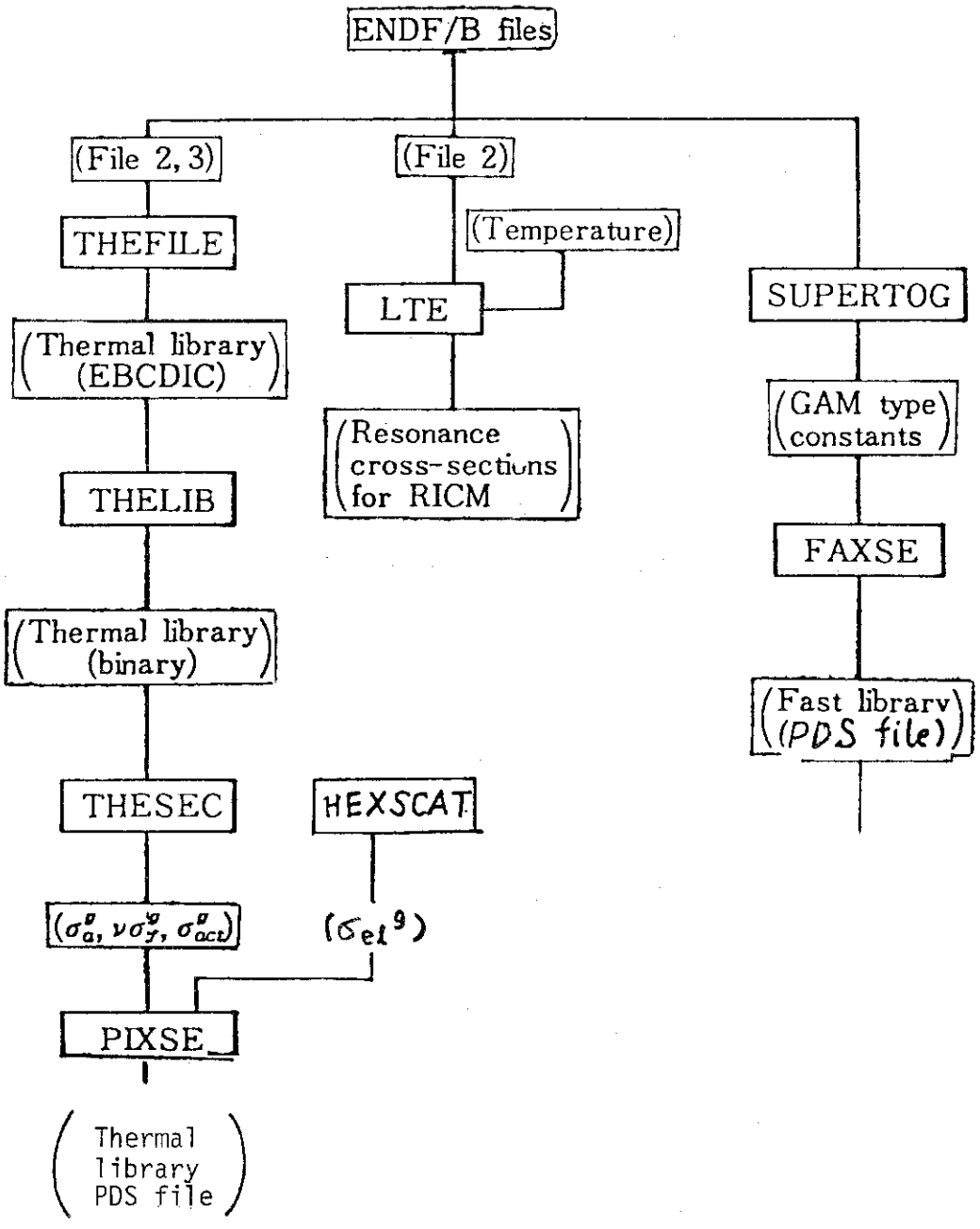

Fig.3.1 Fast and thermal nuclear data handling scheme.

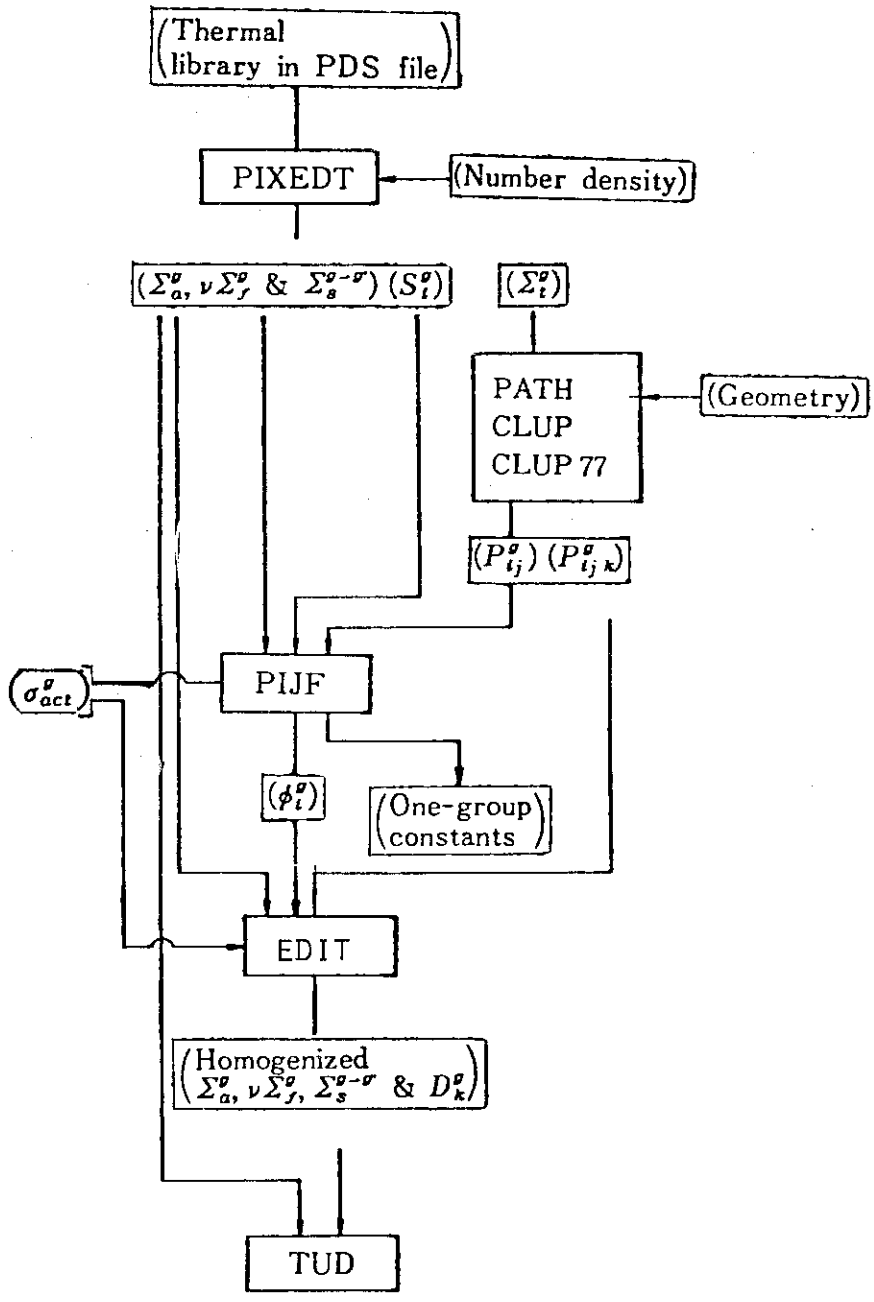

Fig.3.2 Data flow for cell calculation in thermal region.

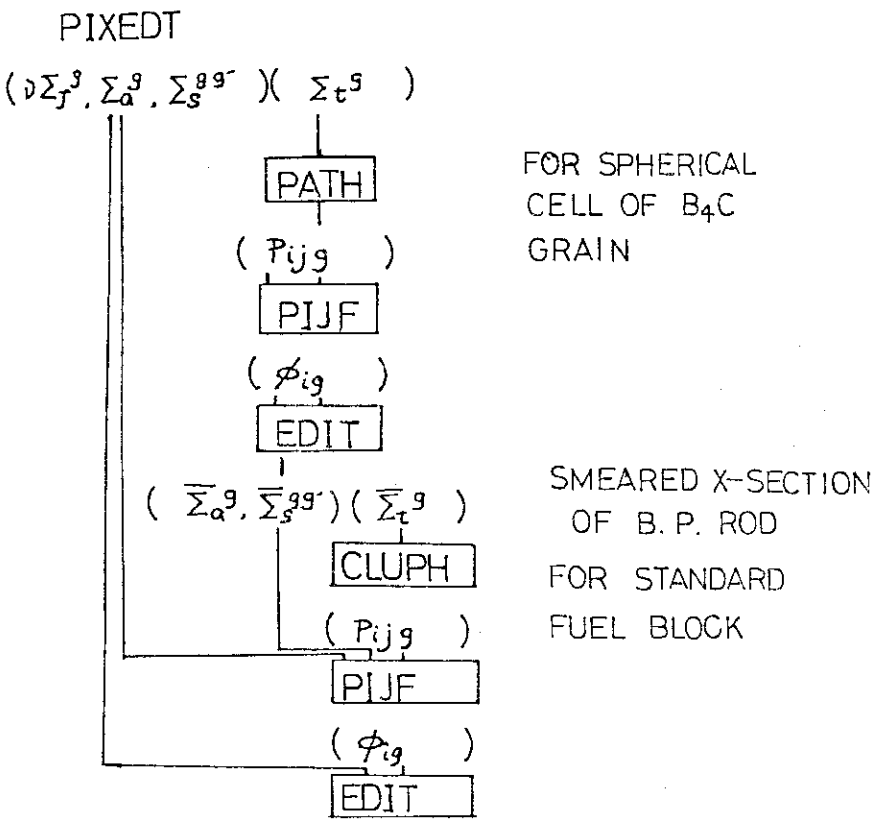

Fig.3.3 Scheme of thermal cell calculation for standard fuel block of VHTR.

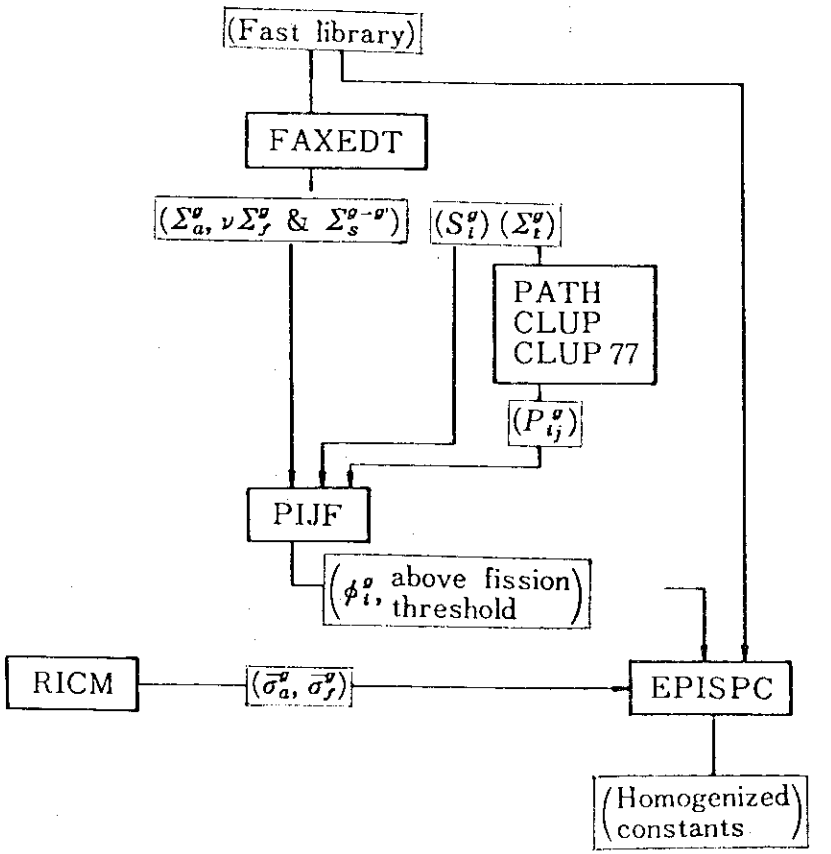

Fig.3.4 Scheme of cell calculation in fast energy region for thermal reactor.

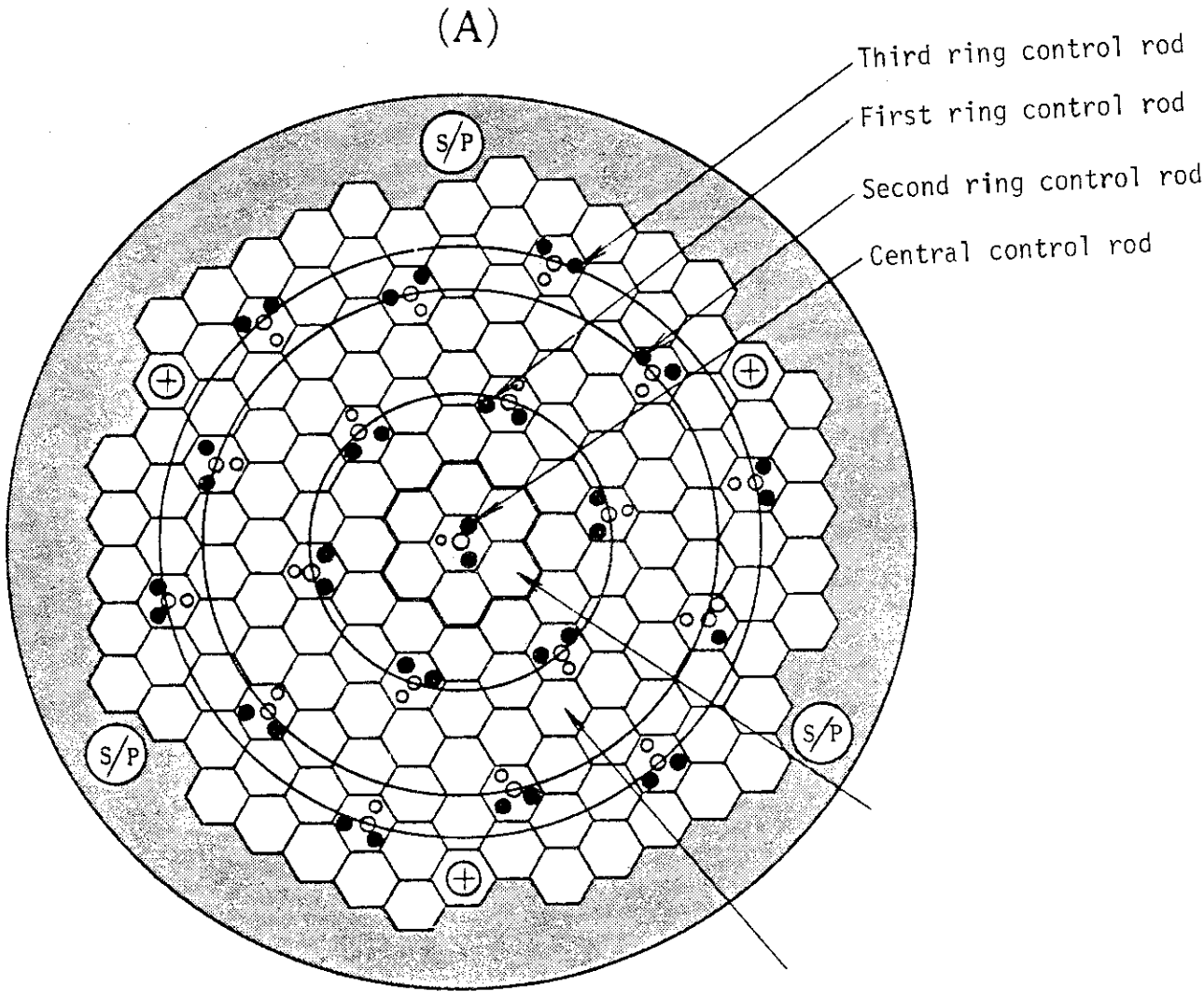

Fig.3.5 Core configuration of VHTR.

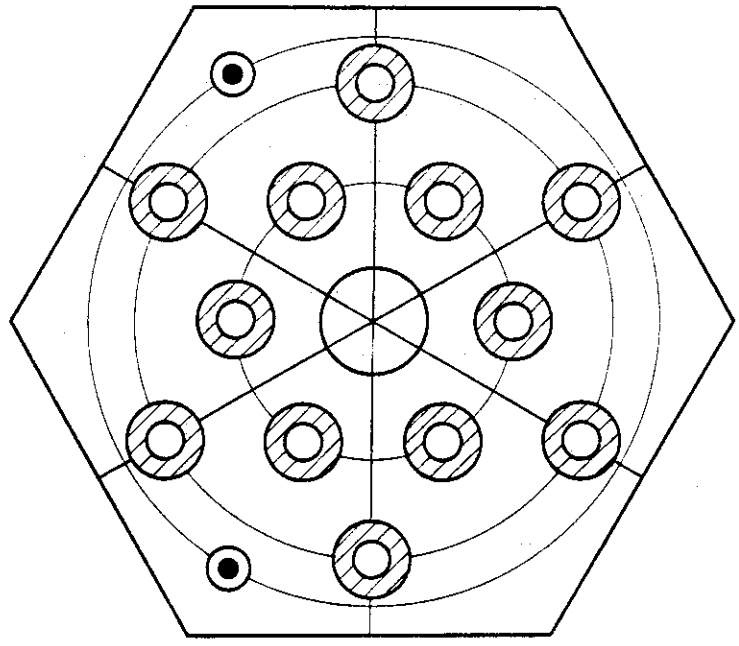

Fig.4.1 Region map of hexagonal cell of MK-III core.

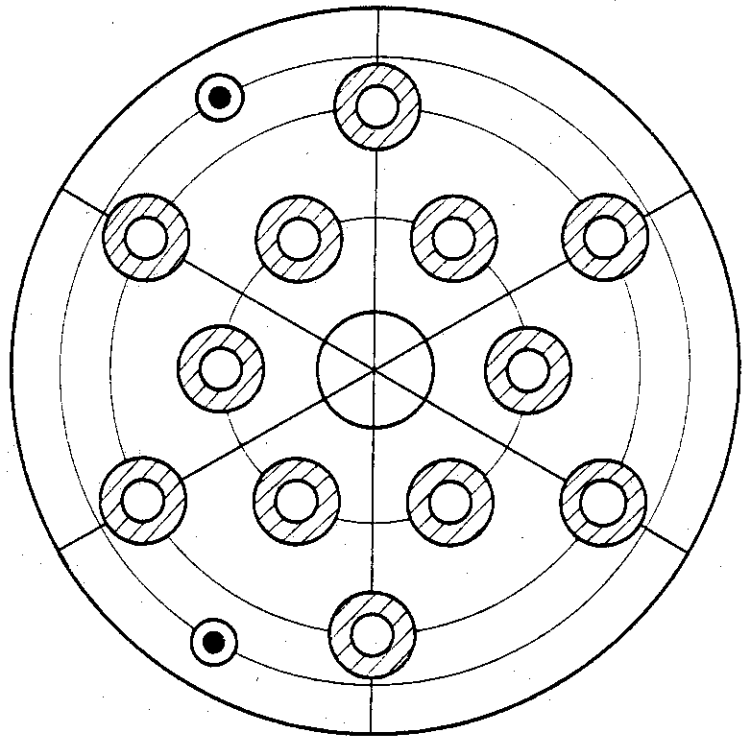

Fig.4.2 Region map of cylindrical cell for MK-III core.

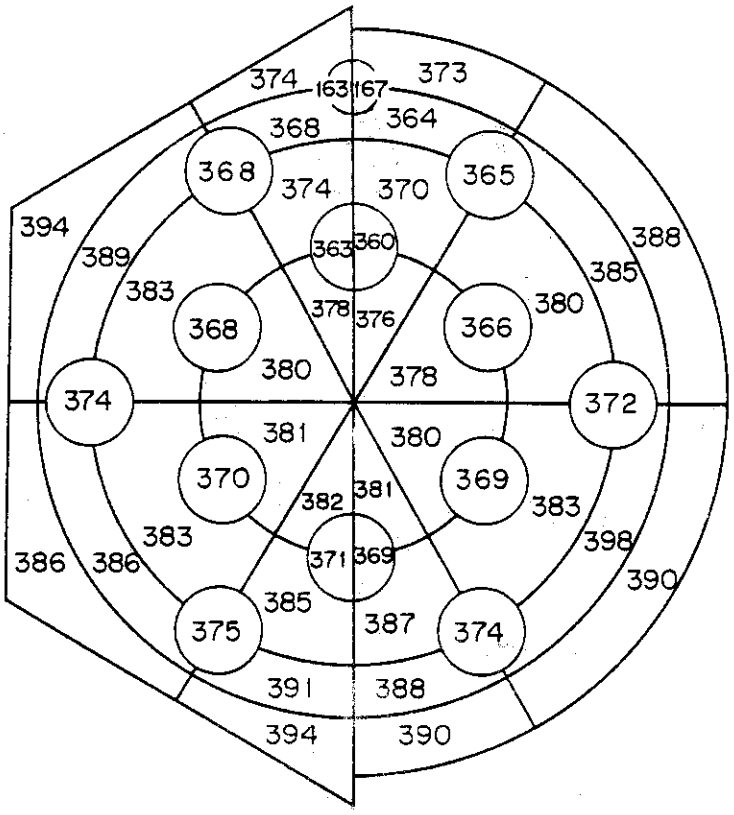

Fig.4.3 Thermal neutron flux in hexagonal fuel block with 2% enriched uranium and a burnable poison rod and in its cylindrical approximation.

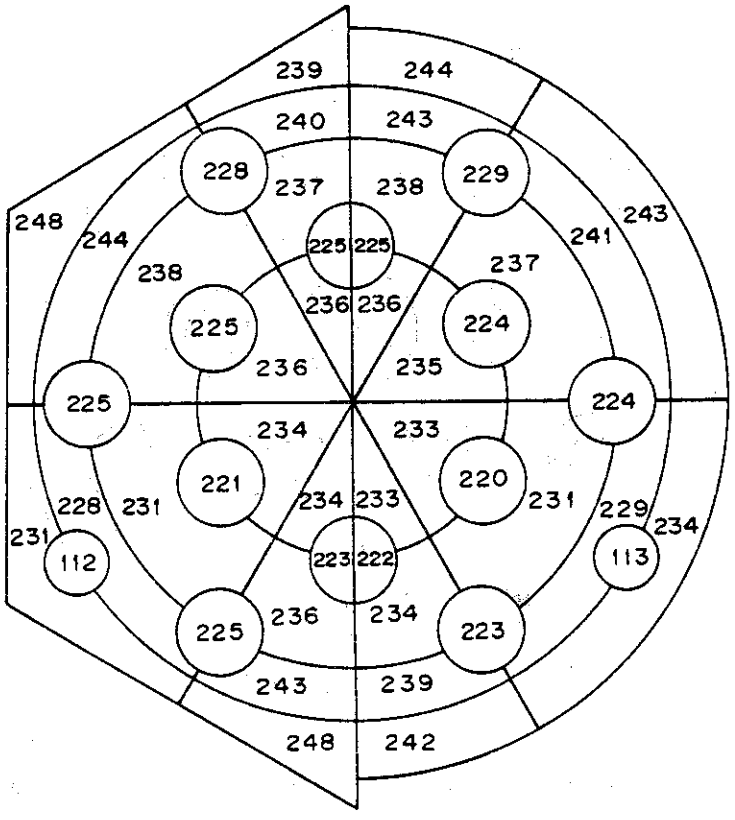

Fig.4.4 Thermal neutron flux in hexagonal fuel block with 4% enriched uranium and two burnable poison rods and in its cylindrical approximation.

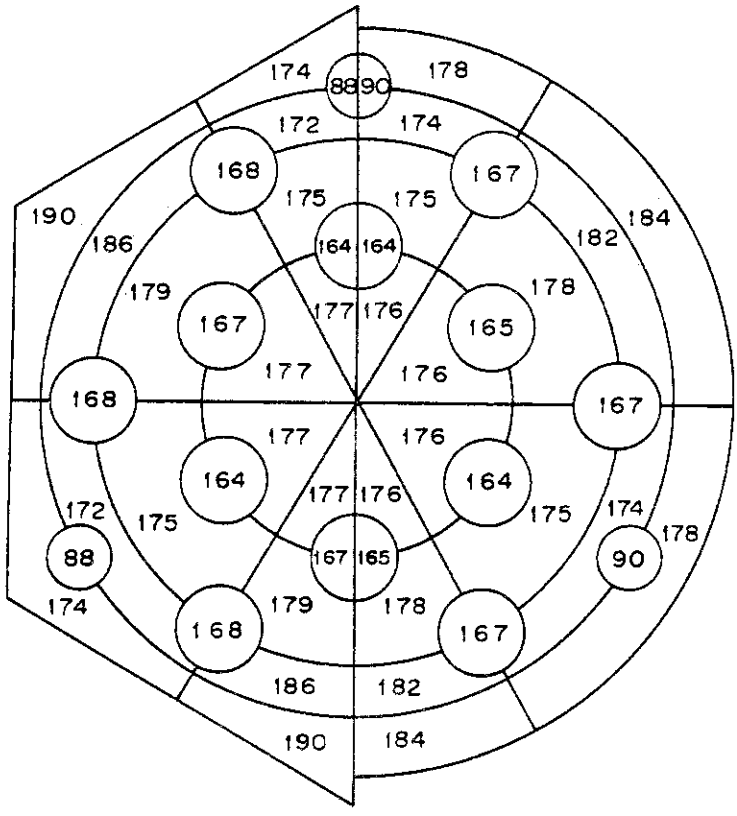

Fig.4.5 Thermal neutron flux in hexagonal fuel block with 6% enriched uranium and three burnable poison rods and in its cylindrical approximation.

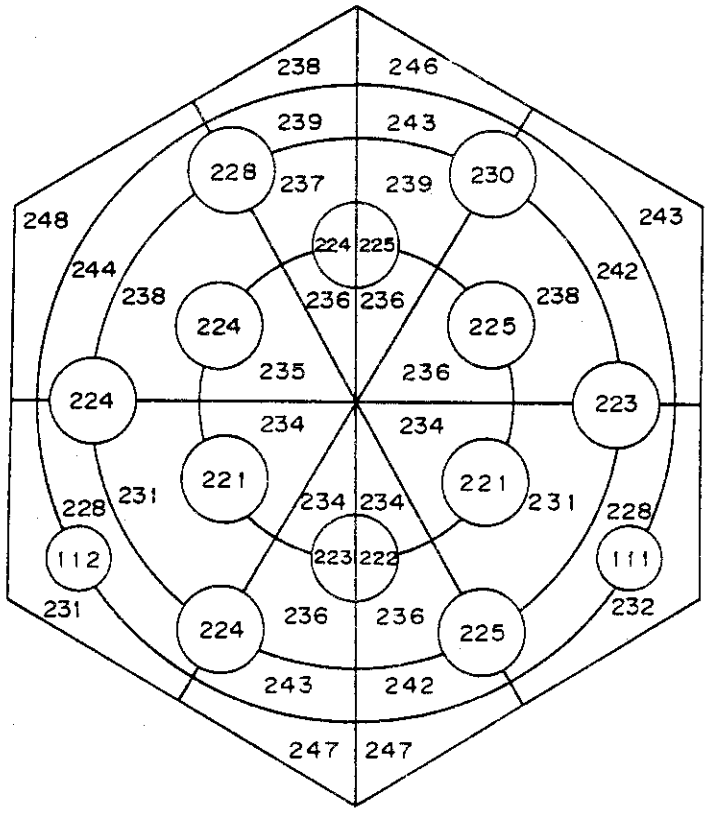

Fig.4.6 Thermal neutron flux calculated by using periodic and rotational array of fuel block with two burnable poison rods.

Table 4.1 Thermal neutron constants of hexagonal and cylindrical cell with 2% enriched uranium and a burnable poison rod.

LATTICE	GRAPHITE CROSS SECTION	ηf	$\nu\Sigma_F$	Σ_{AB}	D
HEXIB	INCOHERENT	1.3155	0.4344×10^{-2}	0.3303×10^{-2}	0.8111
HEXIB	COHERENT	1.3153	0.4345×10^{-2}	0.3304×10^{-2}	0.8364
CLYIB	INCOHERENT	1.3144	0.4344×10^{-2}	0.3305×10^{-2}	0.8111
CLYIB	COHERENT	1.3143	0.4346×10^{-2}	0.3306×10^{-2}	0.8357

Table 4.2 Thermal neutron constants of hexagonal and cylindrical cell with 4% enriched uranium and two burnable poison rods.

LATTICE	GRAPHITE CROSS SECTION	ηf	$\nu\Sigma_F$	Σ_{AB}	D
HEX2B	INCOHERENT	1.4236	0.7599×10^{-2}	0.5338×10^{-2}	0.8152
HEX2B	COHERENT	1.4234	0.7601×10^{-2}	0.5340×10^{-2}	0.8340
CLY2B	INCOHERENT	1.4189	0.7597×10^{-2}	0.5354×10^{-2}	0.8153
CLY2B	COHERENT	1.4188	0.7600×10^{-2}	0.5356×10^{-2}	0.8335
HEX2B (ROTATIONAL)	COHERENT	1.4257	0.7603×10^{-2}	0.5333×10^{-2}	0.8343

Table 4.3 Thermal neutron constants of hexagonal and cylindrical cell with 6% enriched uranium and three burnable poison rods.

LATTICE	GRAPHITE CROSS SECTION	ηf	$\nu\Sigma_F$	Σ_{AB}	D
HEX3B	INCOHERENT	1.4486	0.1030×10^{-1}	0.7110×10^{-2}	0.8172
HEX3B	COHERENT	1.4485	0.1030×10^{-1}	0.7112×10^{-2}	0.8330
CLY3B	INCOHERENT	1.4397	0.1029×10^{-1}	0.7148×10^{-2}	0.8173
CLY3B	COHERENT	1.4396	0.1029×10^{-1}	0.7150×10^{-2}	0.8327

Table 4.4 Thermal neutron constants of standard fuel block with burnable poison rods of B_4C grain structure.

RAIUS OF EQUIVALENT CELL	ηf	$\nu\Sigma_F$	Σ_{AB}	Σ_{AB}(Burnable poison rod)	ρ_B	ρ_{Cl}
0.040(CM)	1.4217	0.7599×10^{-2}	0.5345×10^{-2}	1.728	1.010×10^{-2}	7.135×10^{-2}
0.045	1.4251	0.7602×10^{-2}	0.5334×10^{-2}	1.681	1.438×10^{-2}	6.707×10^{-2}
0.050	1.4298	0.7605×10^{-2}	0.5319×10^{-2}	1.617	1.972×10^{-2}	6.173×10^{-2}
0.060	1.4489	0.7618×10^{-2}	0.5258×10^{-2}	1.442	3.408×10^{-2}	4.737×10^{-2}
0.080	1.4992	0.7657×10^{-2}	0.5107×10^{-2}	1.007	8.079×10^{-2}	6.60×10^{-4}

Table 4.5 Temperature dependence of thermal neutron constants of standard fuel block.

TEMPERATURE (°K)	ηf	$\nu\Sigma_F$	Σ_{AB}	D
296	1.4231	0.7601×10^{-2}	0.5341×10^{-2}	0.8340
400	1.4084	0.7127×10^{-2}	0.5060×10^{-2}	0.8334
800	1.3620	0.5762×10^{-2}	0.4231×10^{-2}	0.8413
1200	1.3331	0.49785×10^{-2}	0.37344×10^{-2}	0.8452

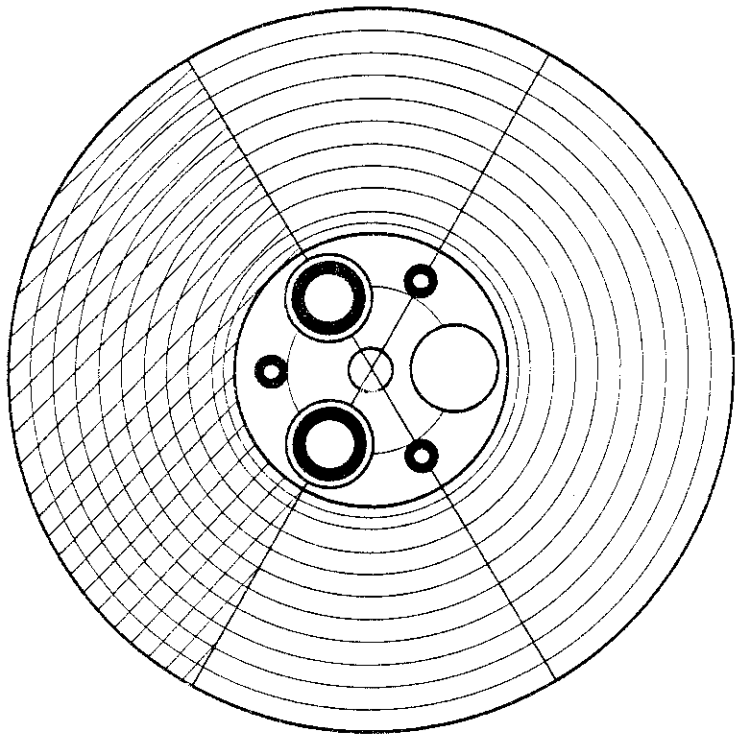

Fig.4.7 Region map of a super cell with control rod block.

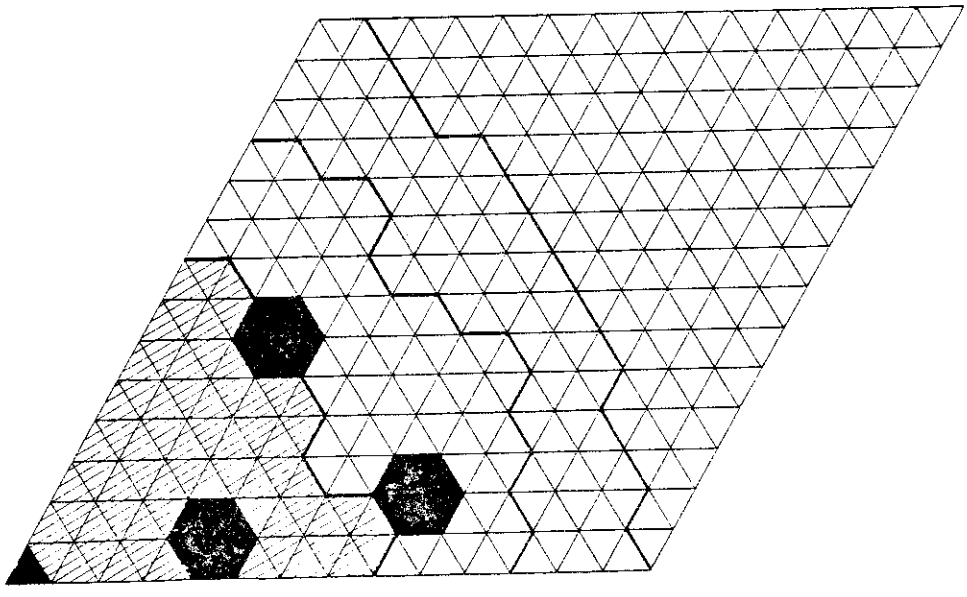

Fig.4.9 1/6 sector of horizontal section of VHTR core.

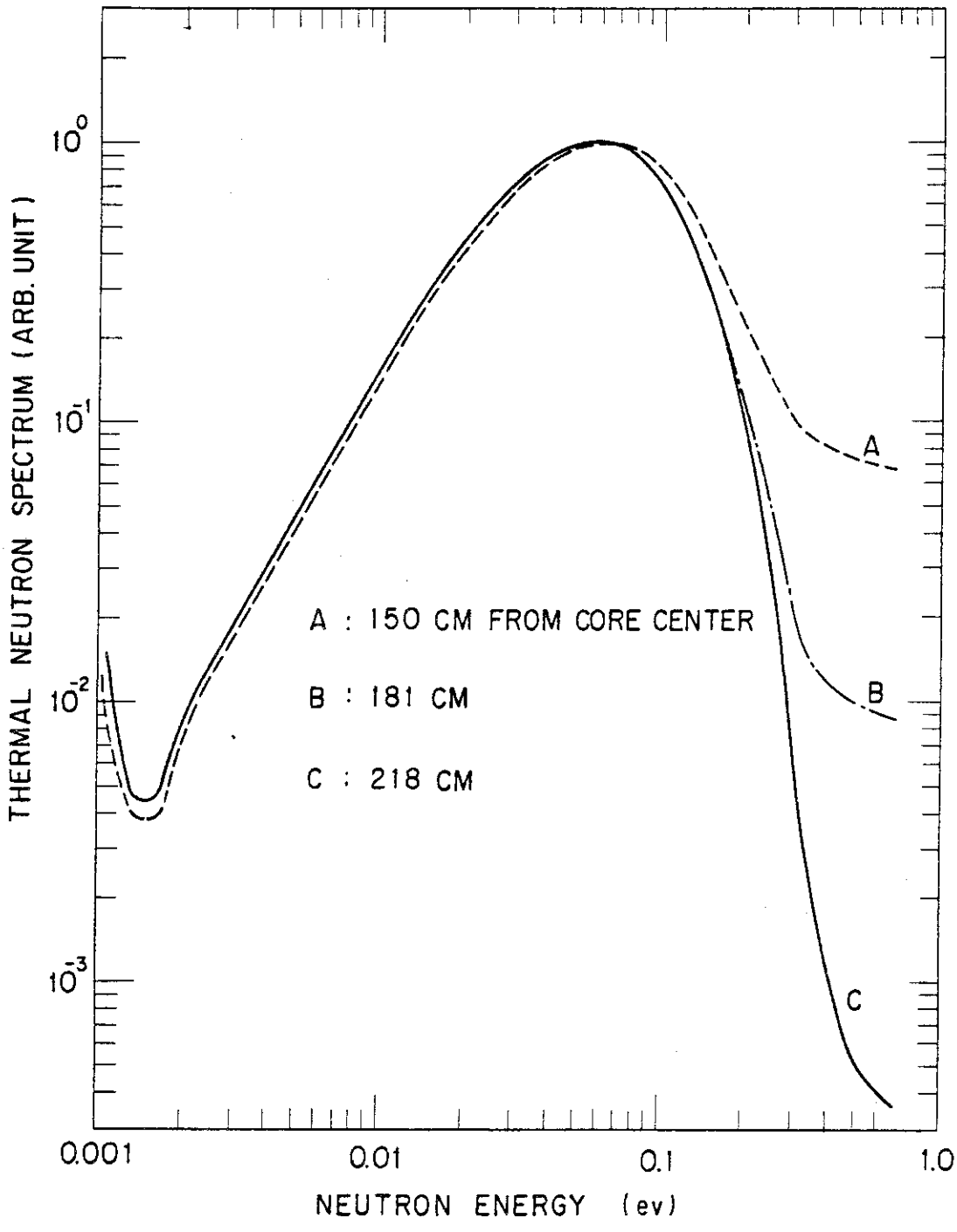

Fig.4.8 Spatial dependence of thermal neutron spectrum in graphite reflector.

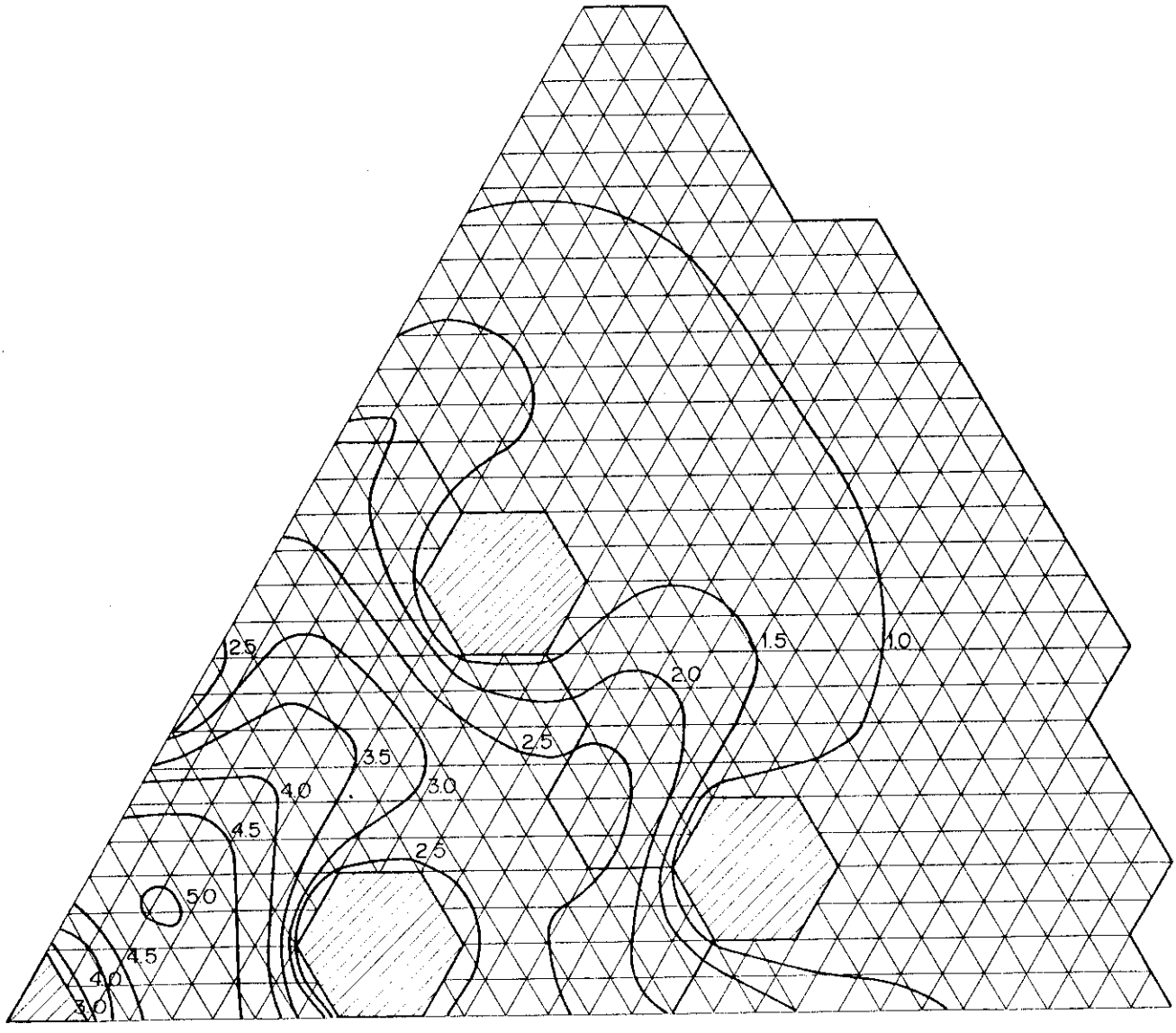

Fig.4.10 Typical neutron flux distribution in 1/6 sector of VHTR core.

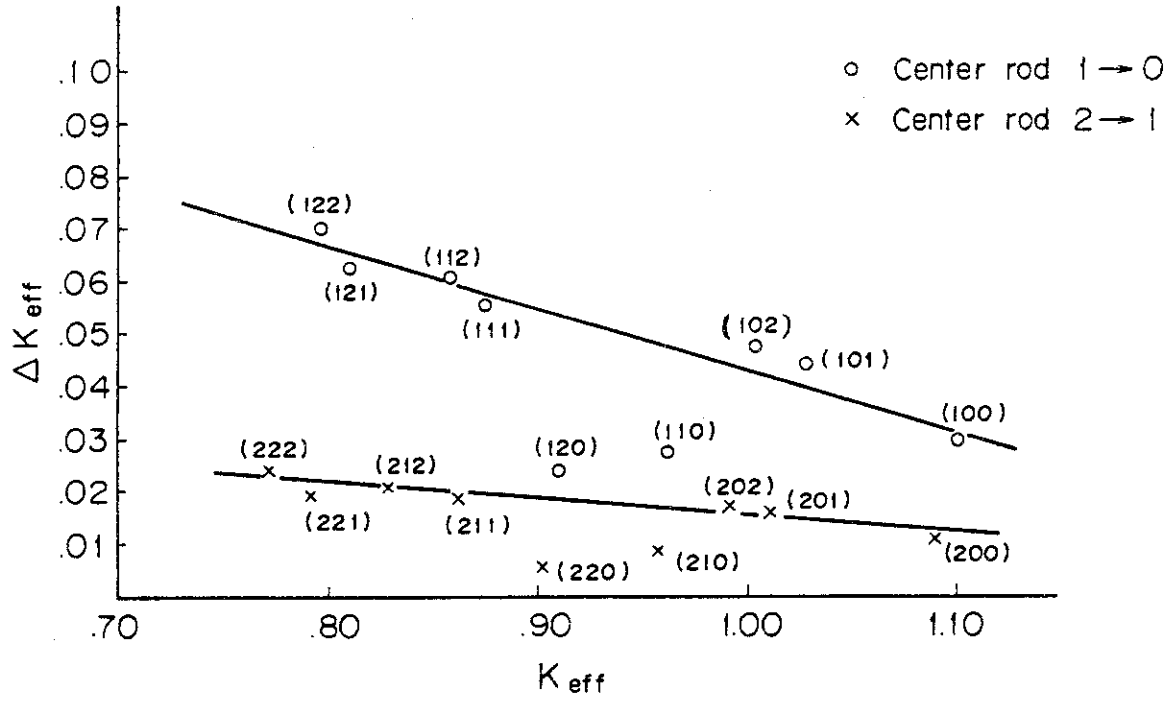

Fig.4.11 Reactivity worth of control rod in central control rod block.

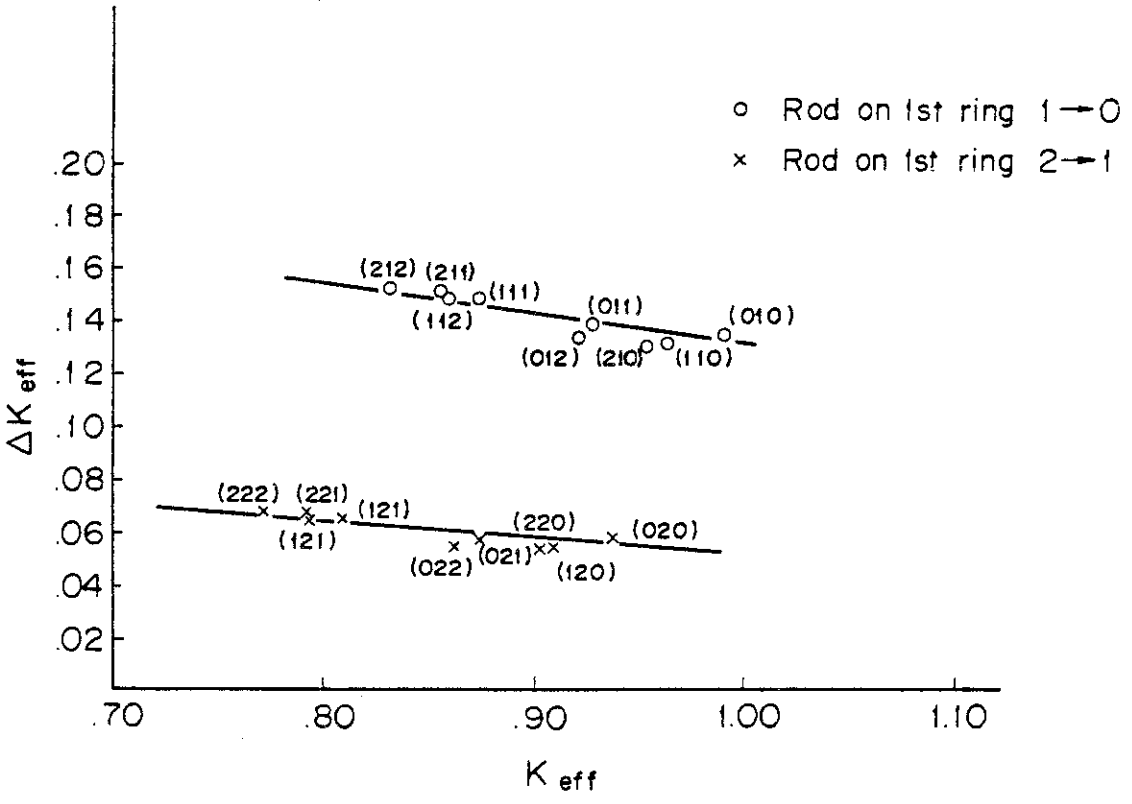

Fig.4.12 Reactivity worth of control rod in first ring control rod block.

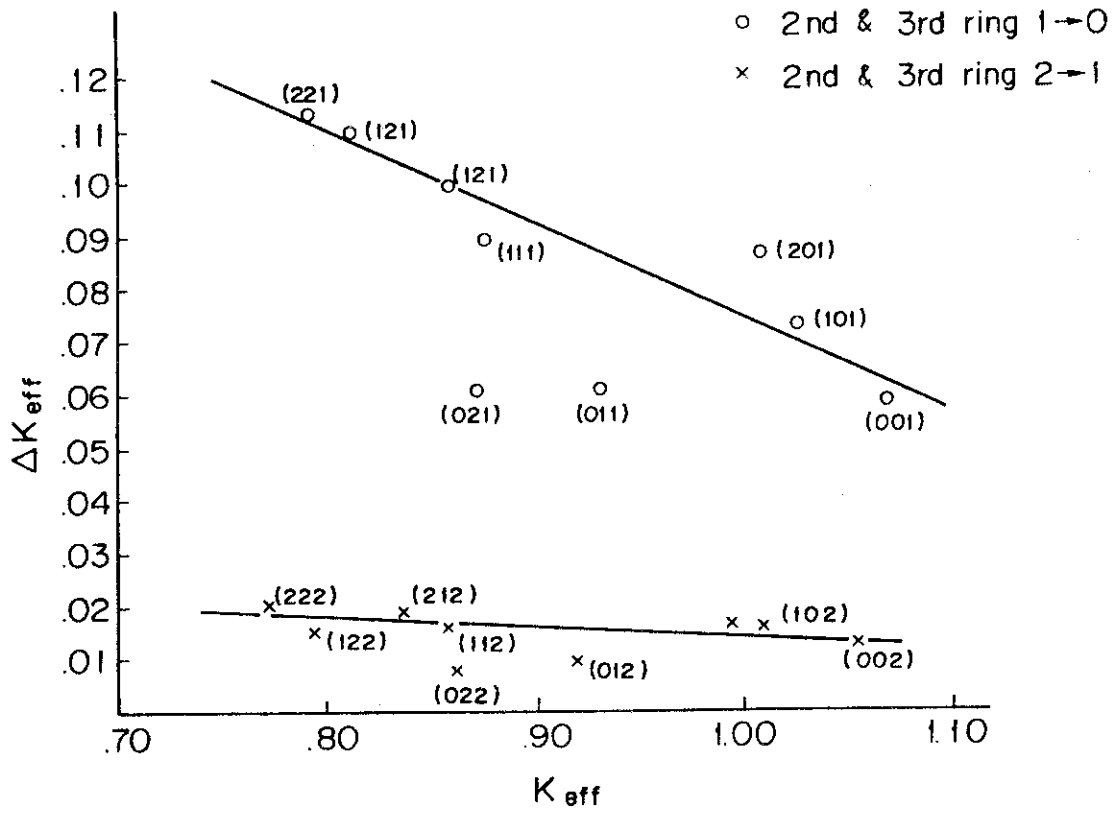

Fig.4.13 Reactivity worth of control rod in second and third ring control rod block.